Fluxnet and regional carbon flux modeling, spatial integration and regional fluxes, spatial scales of coherence, network-scale analysis

Philippe Ciais, Markus Reichstein, Kenneth Davis, Toshinobu Machida, Dario Papale, Galina Churkina, Scott Denning, Gen Inoue, Ivan Janssens, Natasha Miles, et al.

Fluxnet and regional carbon flux modeling

(spatial integration and regional fluxes, spatial scales of coherence, network-scale analysis),

Ph. Ciais, M. Reichtein, K. Davis, T. Machida, D. Papale, S. Arshimov, G. Churkina, S. Denning, G. Inoue, I. Janssens, N. Miles, S. Richardson, K. Trusilova, R. Valentini, N. Viovy, A. Granier [4], J. Ogée [5], V. Allard [6], M. Aubinet [7] , Chr. Bernhofer [8], A. Carrara [9], F. Chevallier [1], N. De Noblet [1], A. Friend [1], T. Grünwald [8], B. Heinesch [7], P. Keronen [10], A. Knohl [11,12], D. Loustau [5], G. Manca [2], G. Matteucci [13], F. Miglietta [14], J.M. Ourcival [15], K. Pilegaard [16], S. Rambal [15], G. Seufert [13], J.-F. Soussana [6], M.-J. Sanz [9], E.D. Schulze [11], T. Vesala [10]

Estimating regional fluxes

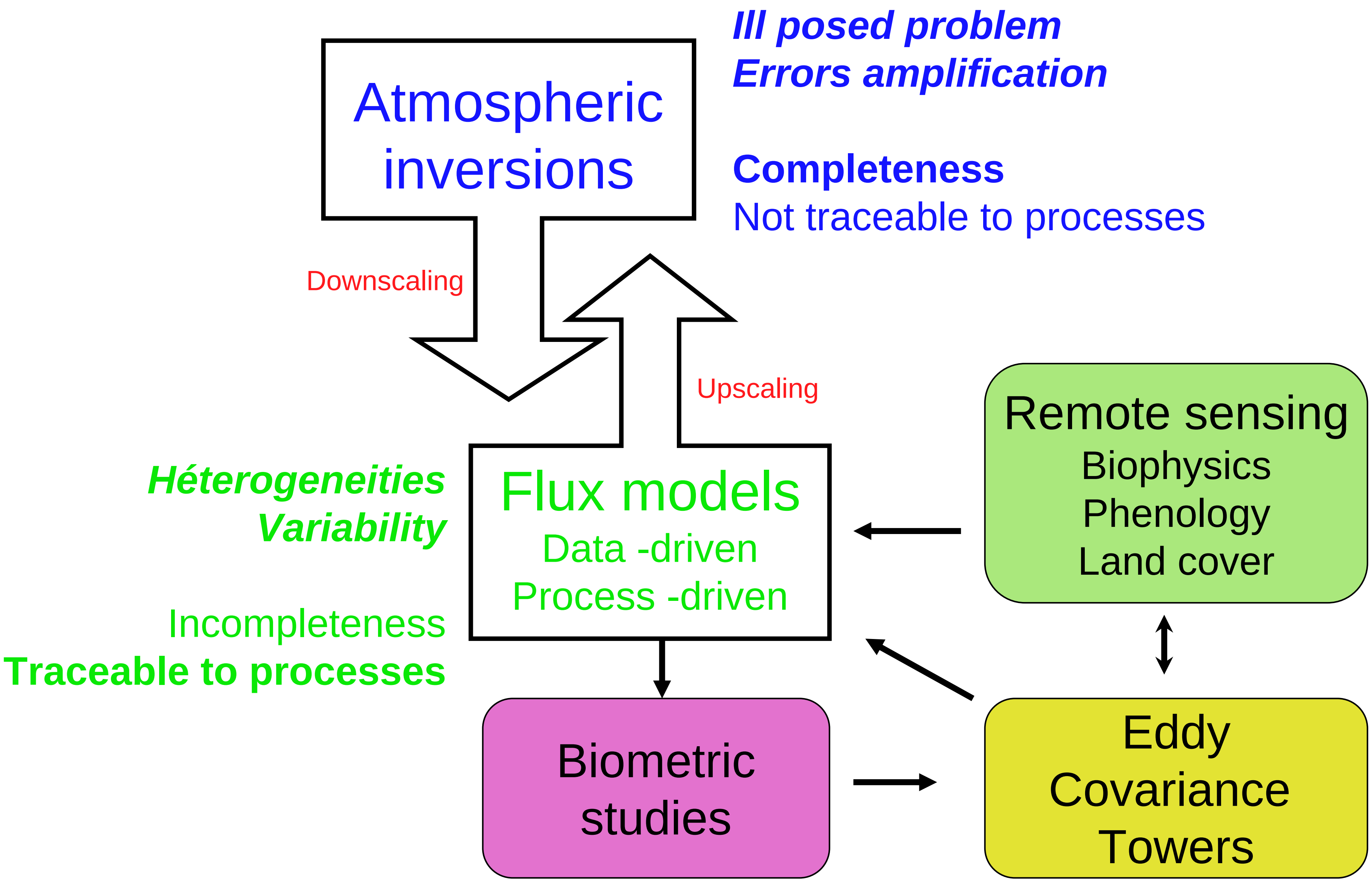

Inversions

Forward model

$$S \;-\; \nabla \bullet (\rho\, C\, \vec{V}) \;=\; \frac{\partial}{\partial t}(\rho\, C)$$

Sources
x_b + *errors*

transport
H

Simulated Concentrations

Observations
y_o + *errrrs*

Inversion

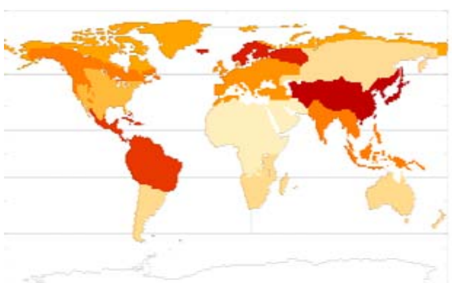

$$\mathbf{H\,x = y}$$

Flux estimate x_a which produces the best fit the atmospheric data

Estimation : $x_a = x_b + \left(H^T R^{-1} H + P^{-1}\right)^{-1} H^T R^{-1} (y_0 - H x_b)$

Error : $P_a = (H^t R^{-1} H + P^{-1})^{-1}$

Joint constraints! Complementary methods : 1. Continental budgets

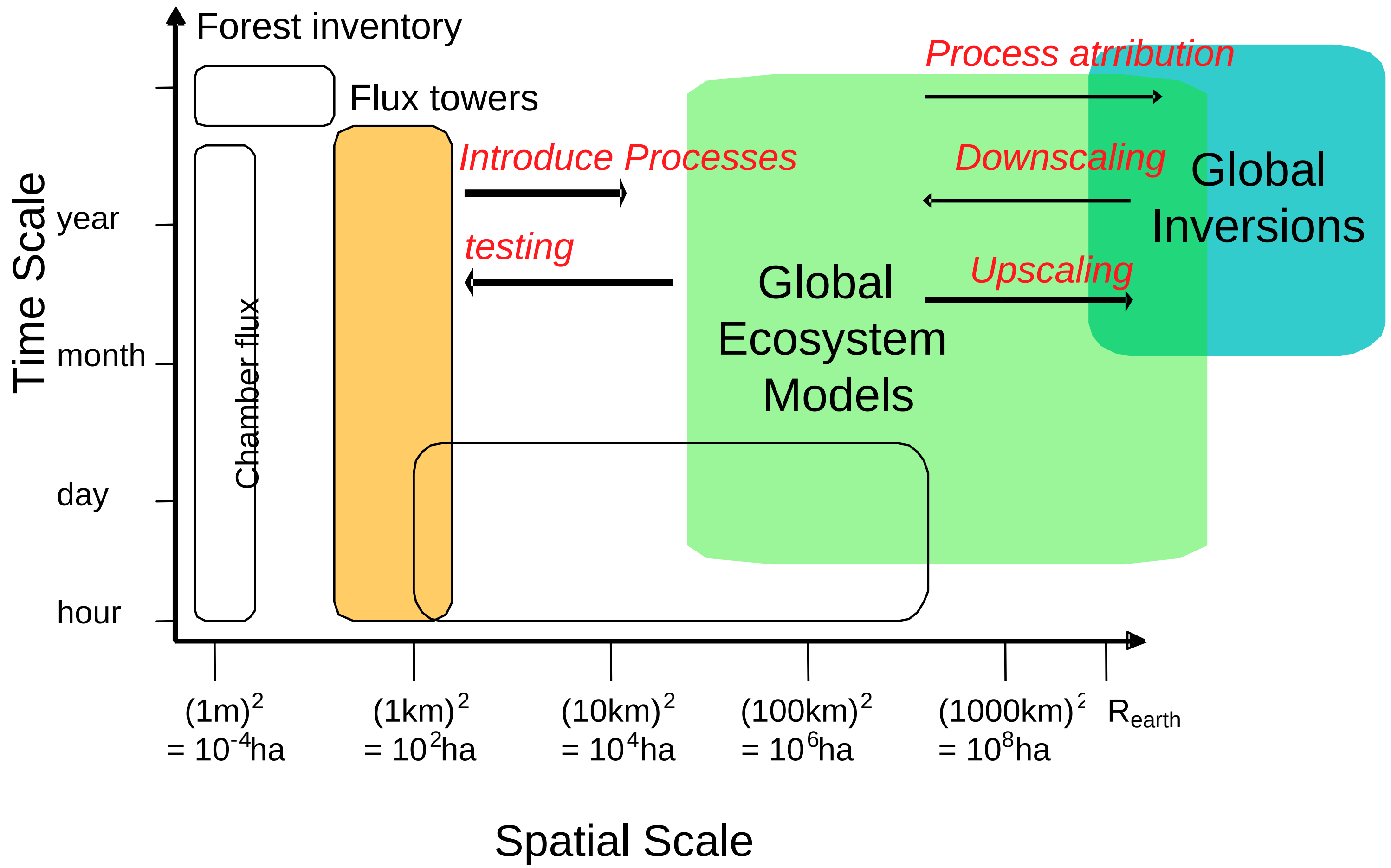

Inversion of Continental Fluxes

Sources of uncertainties

- Data errors
- Network density
- Transport biases
  seasonal vertical advection
- Inversion set-up
  Prior flux aggregations
  Prior errors
  Prior estimate

Apportionment of NH sink in longitude

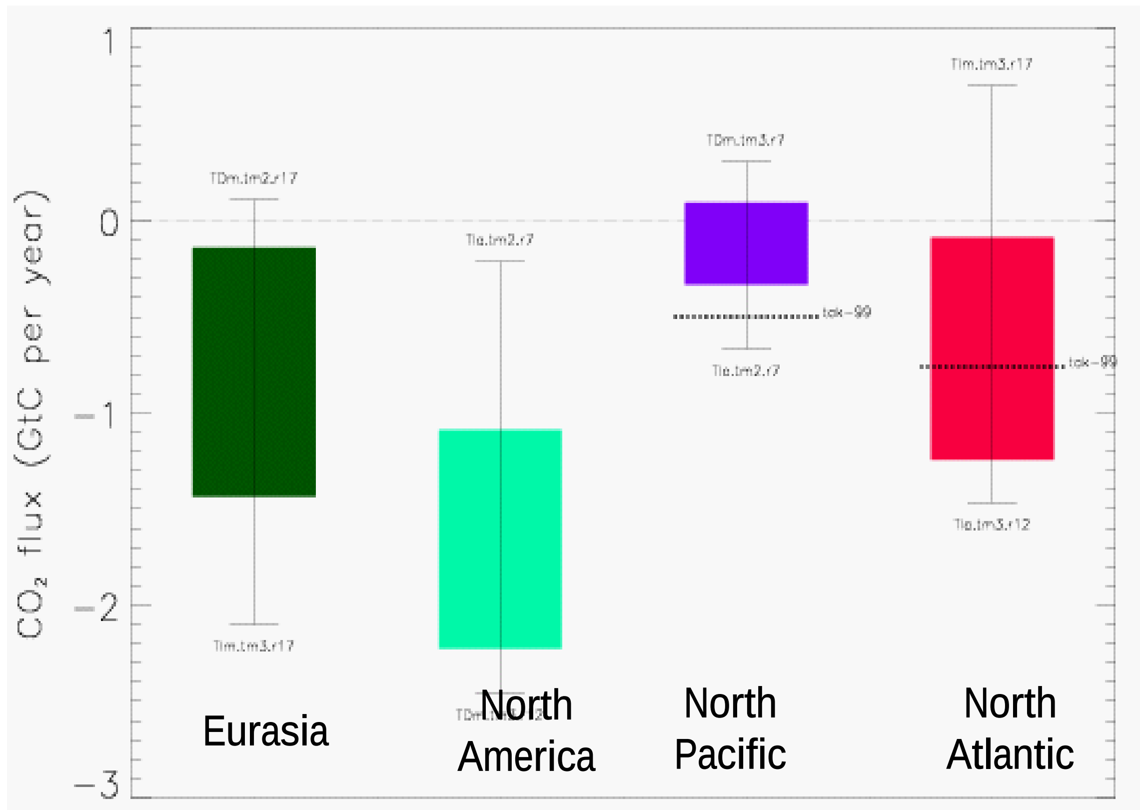

Peylin et al. (2002)

Interannual variations in CO_2 growth rate

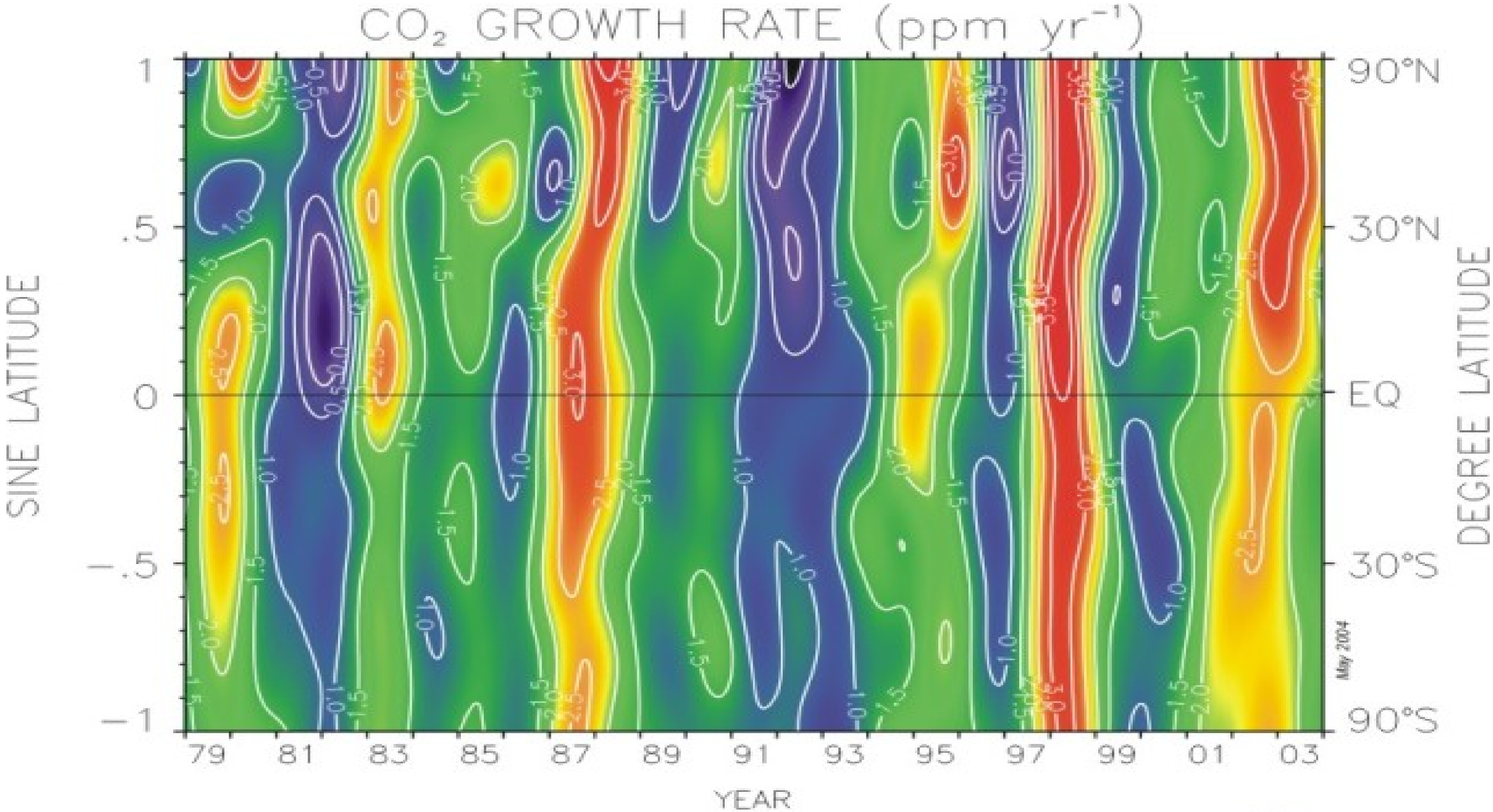

Contour plot showing the temporal and spatial variations in the atmospheric increases of carbon dioxide. The cooler colors (green, blue, violet) represent periods of lower than average growth rates and the warmer colors (yellow, orange, red) represent high growth rate periods. The plot is derived from measurements of thousands of samples collected at the CMDL cooperative air sampling network sites. The variations in the growth rate of this climatically important gas are due to interannual variations in the imbalance between sources and sinks, and also to variations in atmospheric transport. Principal investigator: Thomas Conway, NOAA CMDL Carbon Cycle Greenhouse Gases, Boulder, Colorado, (303) 497-6681 (thomas.j.conway@noaa.gov, http://www.cmdl.noaa.gov/ccgg).

IAV of global fluxes

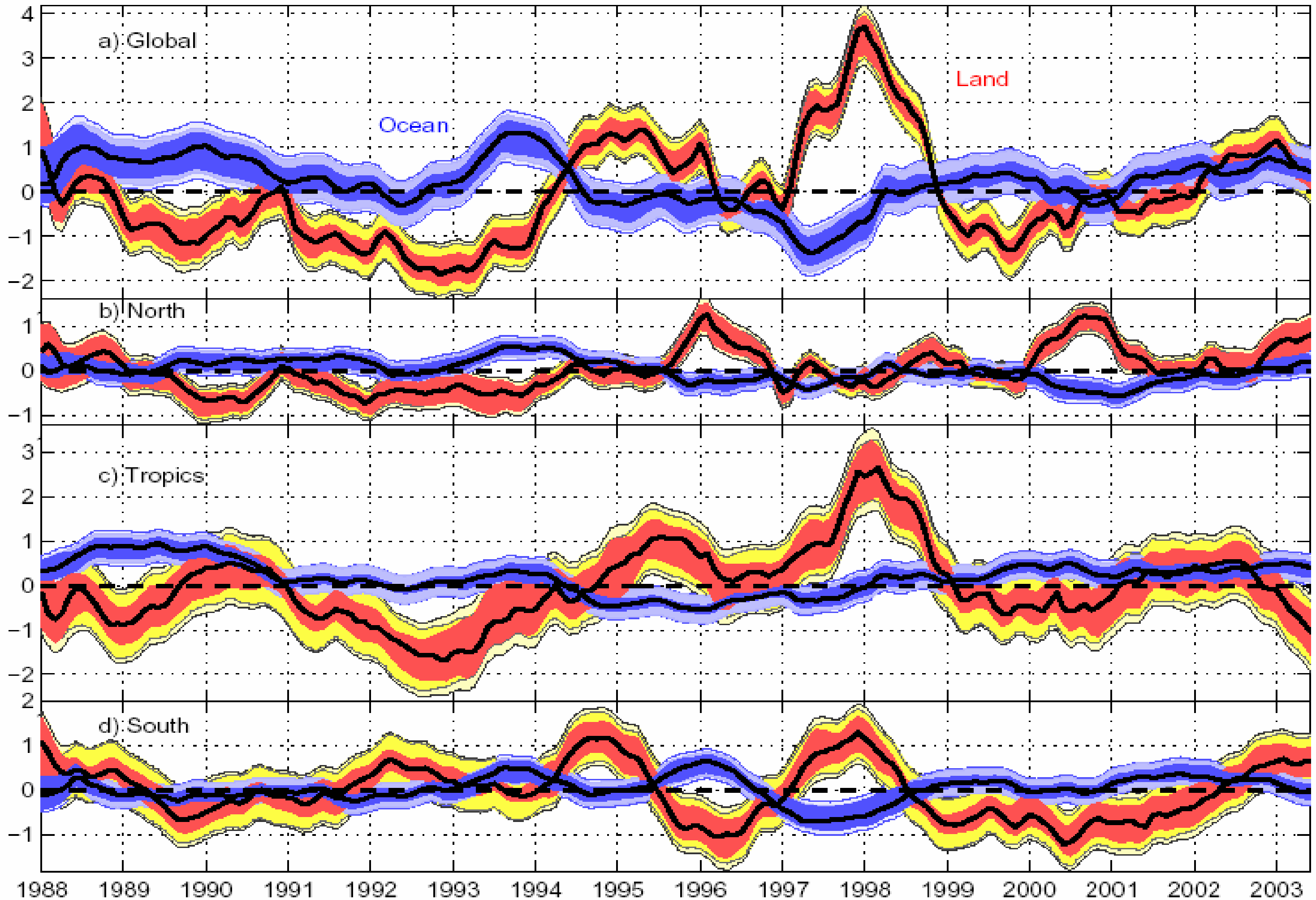

Figure 4. The land and ocean flux interannual variability (PgC yr^{-1}) from x^{IAV} for the full globe, and for the three broad latitude bands defined in Table 4.

Backer et al. (2004) subm.

IAV of Continental scale fluxes

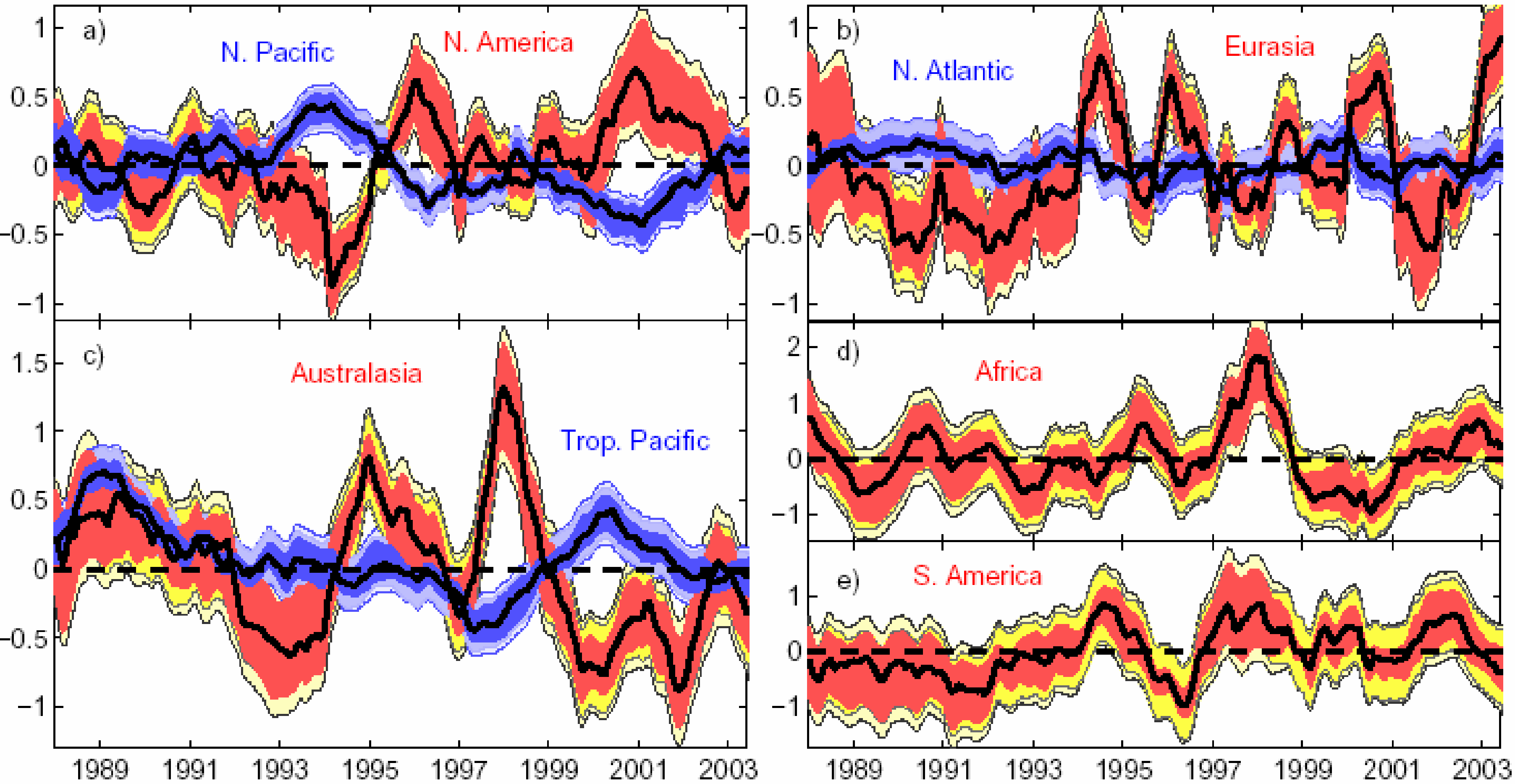

Figure 5. The 13-model mean CO_2 flux IAV [PgC yr^{-1}] from x^{IAV} on the continent/basin scale for the regions defined in Table 4: a) North Pacific & North America, b) North Atlantic & Eurasia, c) Australasia & Tropical Pacific, d) Africa, and e) South America (note the different scales for Africa and S. America).

Joint constraints! Complementary methods : 2. sub-continental budgets

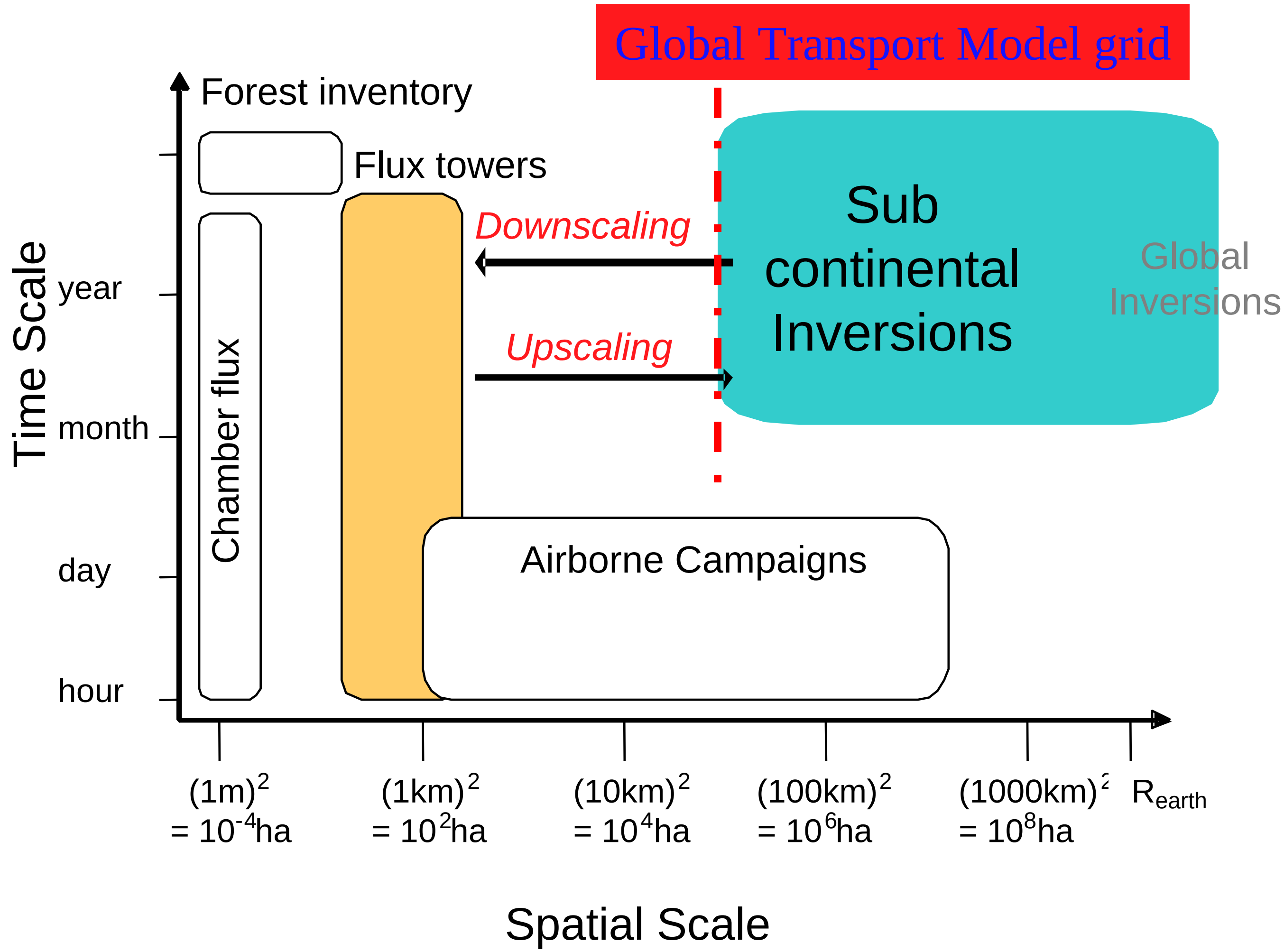

Inversions on the model grid

Regional scale Fluxes from continuous CO_2 concentrations

Daily fluxes over Europe at 50 km

(over the rest of globe (large regions)

Sources of Uncertair

- Transport
  Synoptic horizontal
  Diurnal vertical
- Prior Fluxes
  Scales of coherence
  Diurnal Cycle
  Synoptic variability
- Representiveness
- Network density

Flux correction

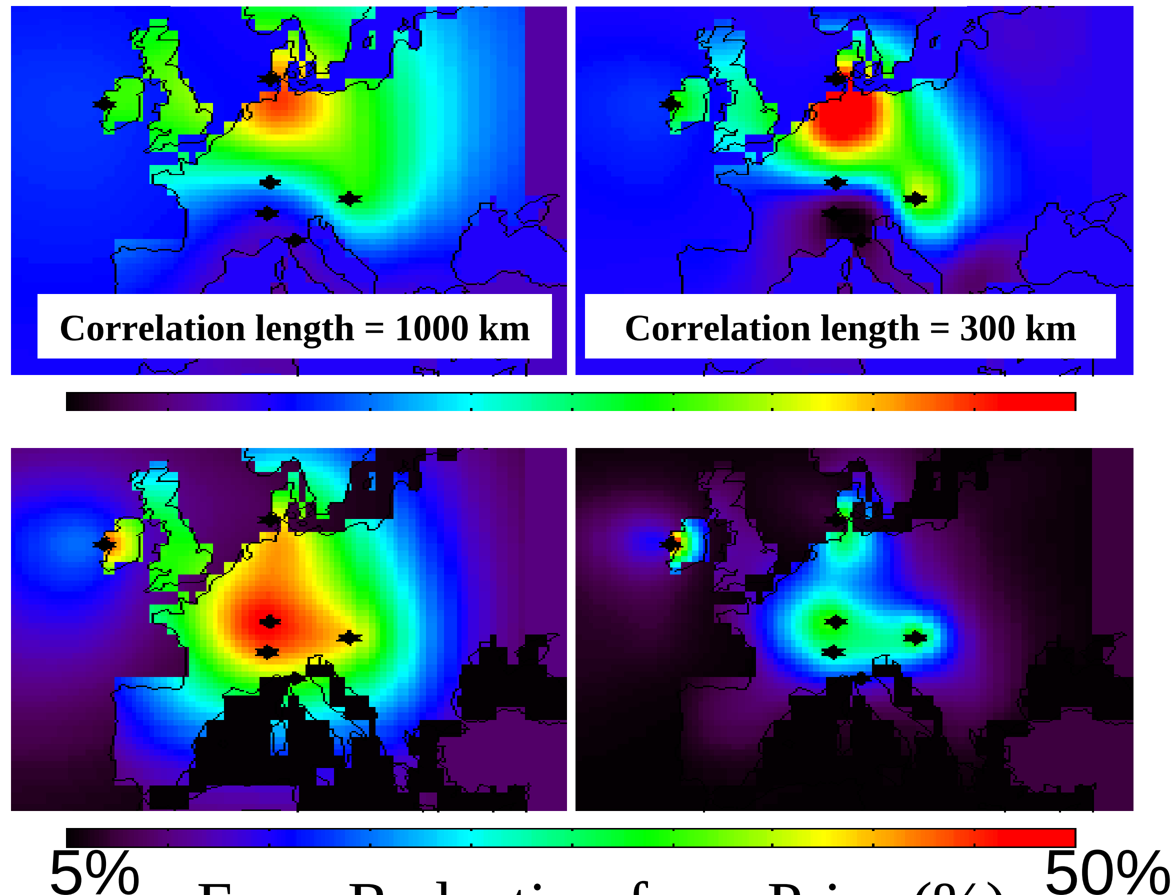

Error Reduction from Prior (%)

Carouge et al. 2004

NOAA CMDL Carbon Cycle Greenhouse Gases
MEASUREMENT PROGRAMS - 2007

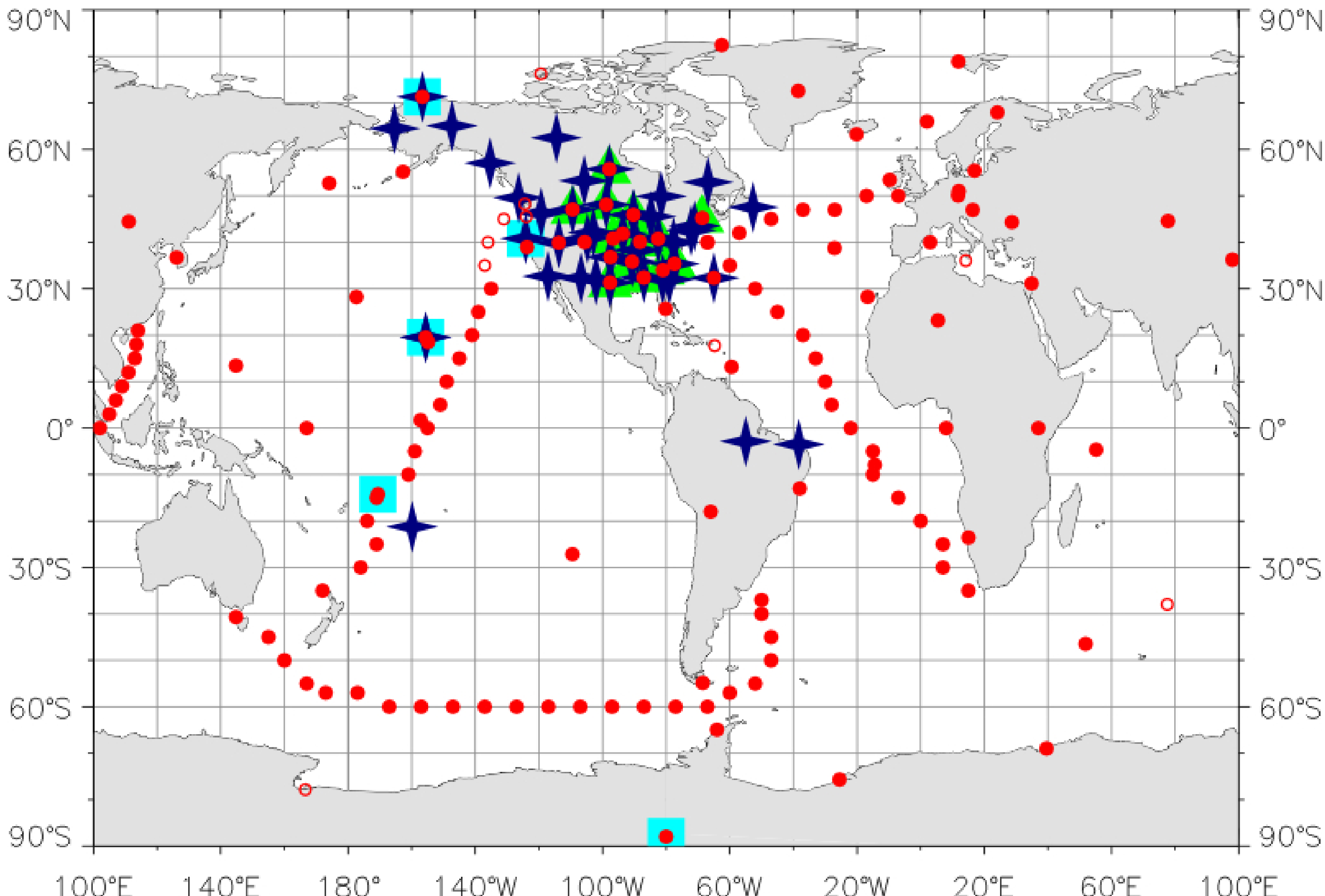

Linking bottom up observations ?
A 2003 European heatwave case study

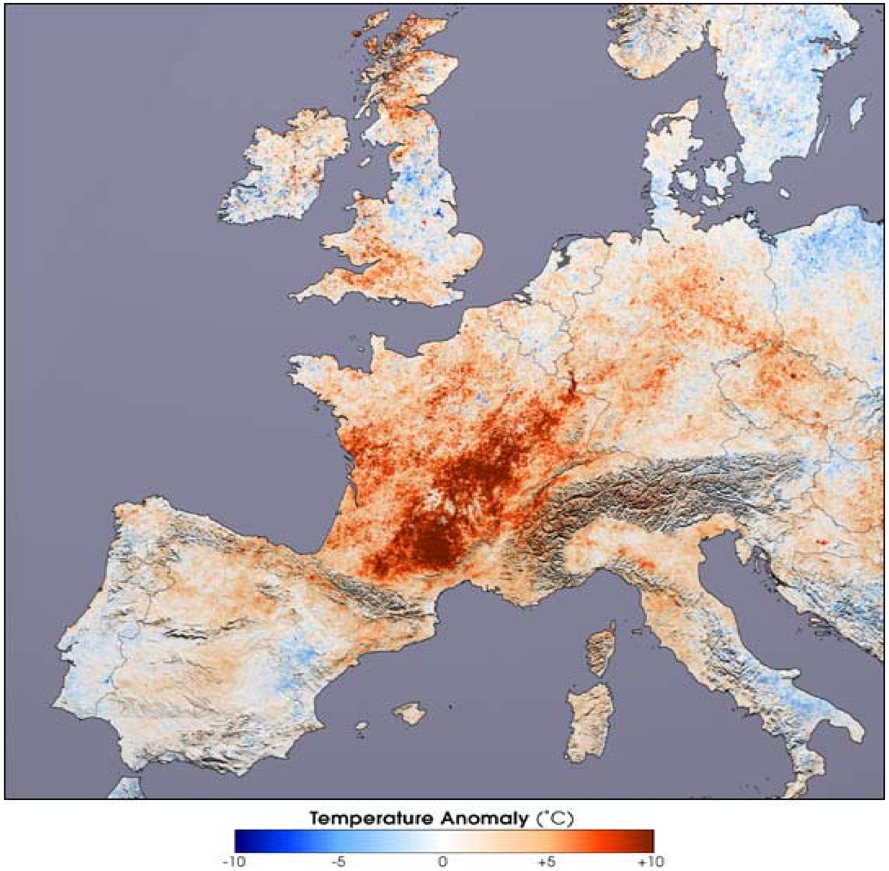

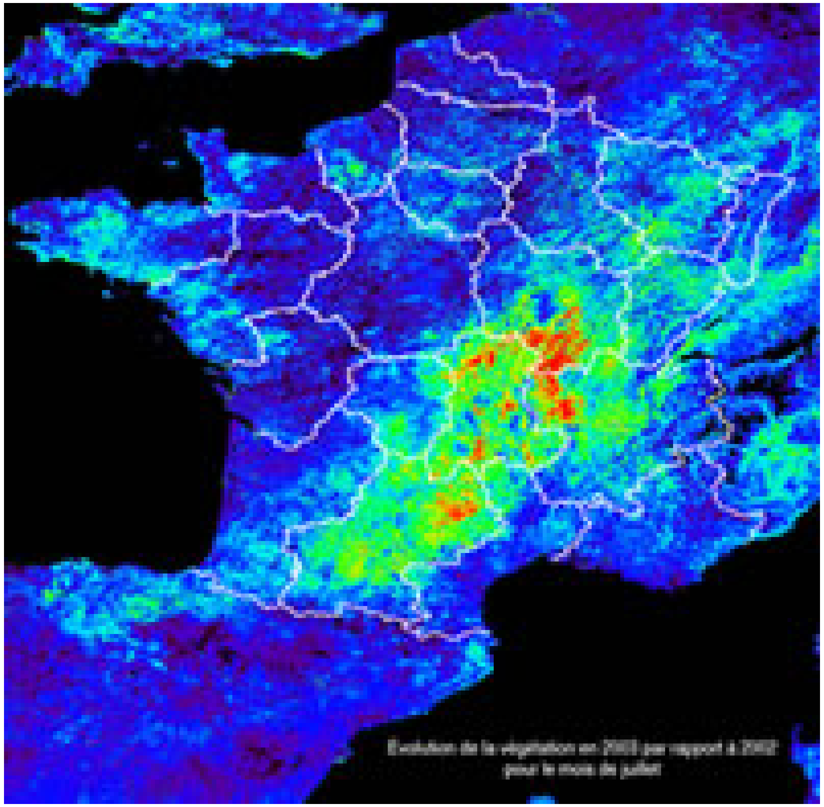

Secular increase in primary productivity from satellite NDVI over the past 25 years

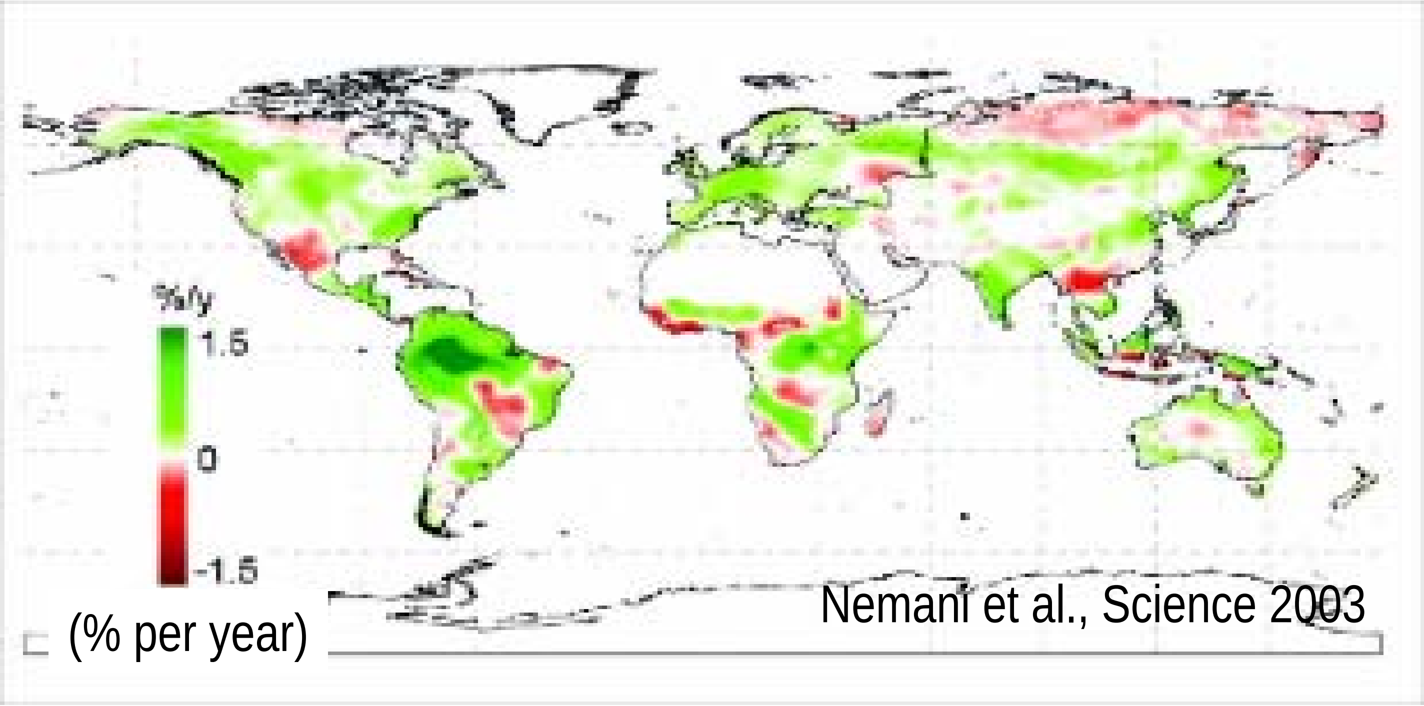

Will the greening continue if more frequent climate extremes impact productivity and net fluxes ?

Historical temperature records in Switzerland

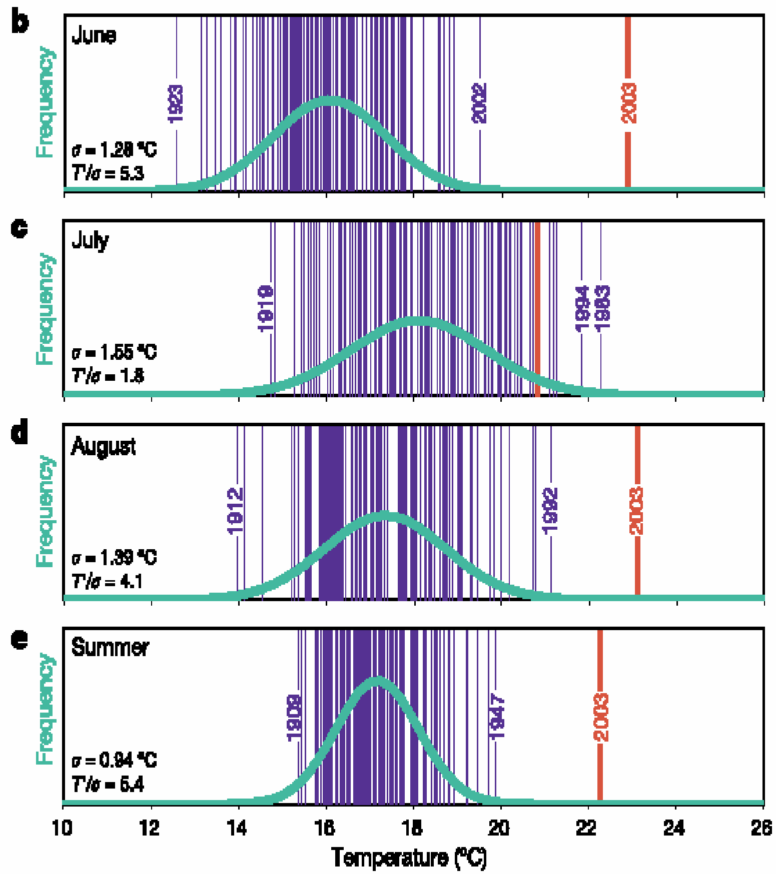

Shär et al., Nature 2003

Precipitation history in Bavaria

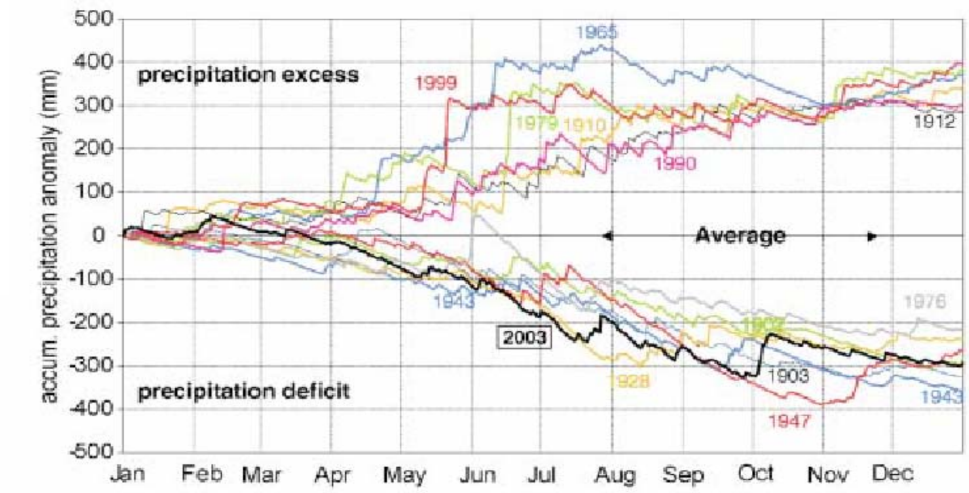

Summer temperature reconstruction from harvest dates in Burgundy

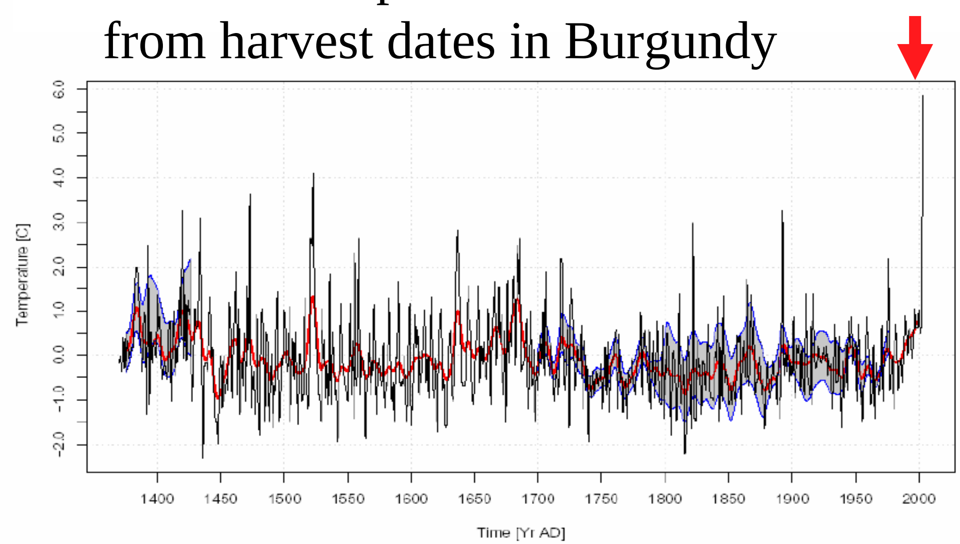

Chuine et al., Nature, 2004

Integrating Regional Carbon Budgets

- Eddy covariance fluxes
- Crop yield statistics
- Remote sensing
- Atmospheric concentration
- Tree rings
- Terrestrial ecosystem models

Multiple Constraint Observations

	Spatial representativity	Temporal resolution	Information on processes	Long term record
Flux Towers Network	- - (++ from processes and network)	+++	+++	-
Crop yields	+ Averaged at the resolution of yield data	--	---	+++
Remote sensing	+++ But only GPP, NPP	+++ But only GPP, NPP	-	+ From different sensors

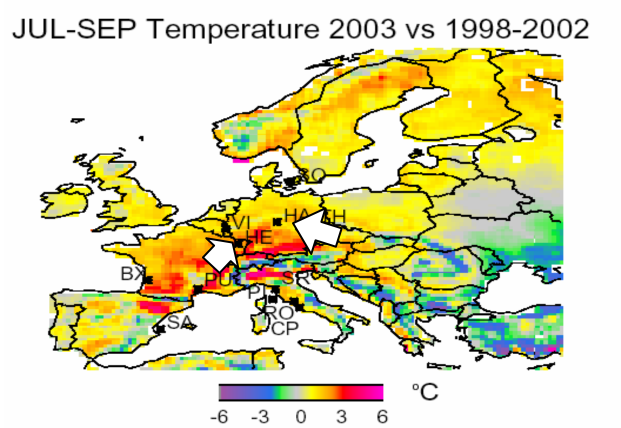

Two Beech forests

Hainich

Eastern Germany

150 years

Hesse

Eastern France

30 yrs

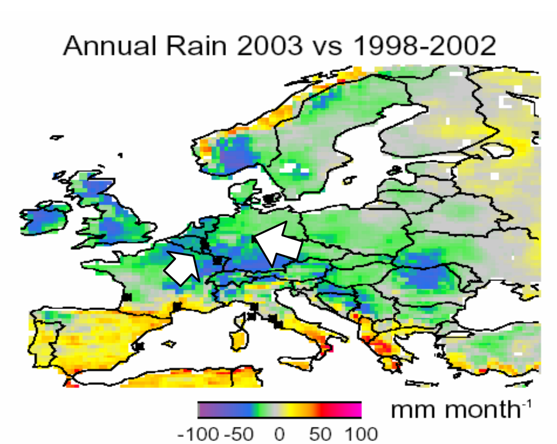

QuickTime™ et un
décompresseur TIFF (LZW)
sont requis pour visionner cette image.

Mediterranean forests

Holm oak Maquia Oak Pine

QuickTime™ et un
décompresseur TIFF (LZW)
sont requis pour visionner cette image.

QuickTime™ et un
décompresseur TIFF (LZW)
sont requis pour visionner cette image.

Annual GPP and TER ...

are coupled... ... and even the difference 2003-2002.

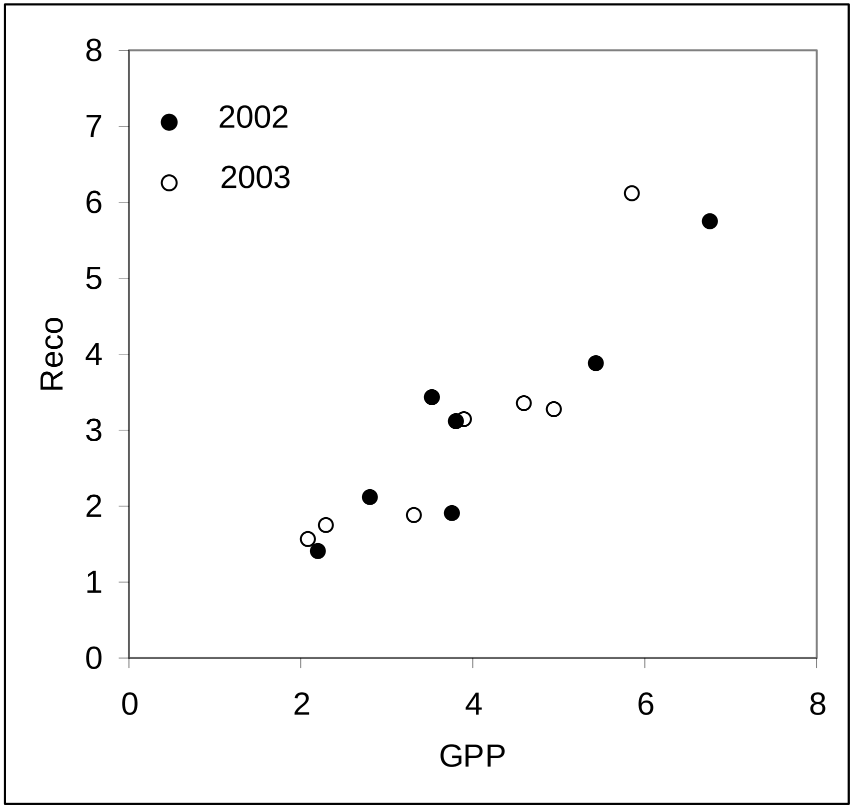

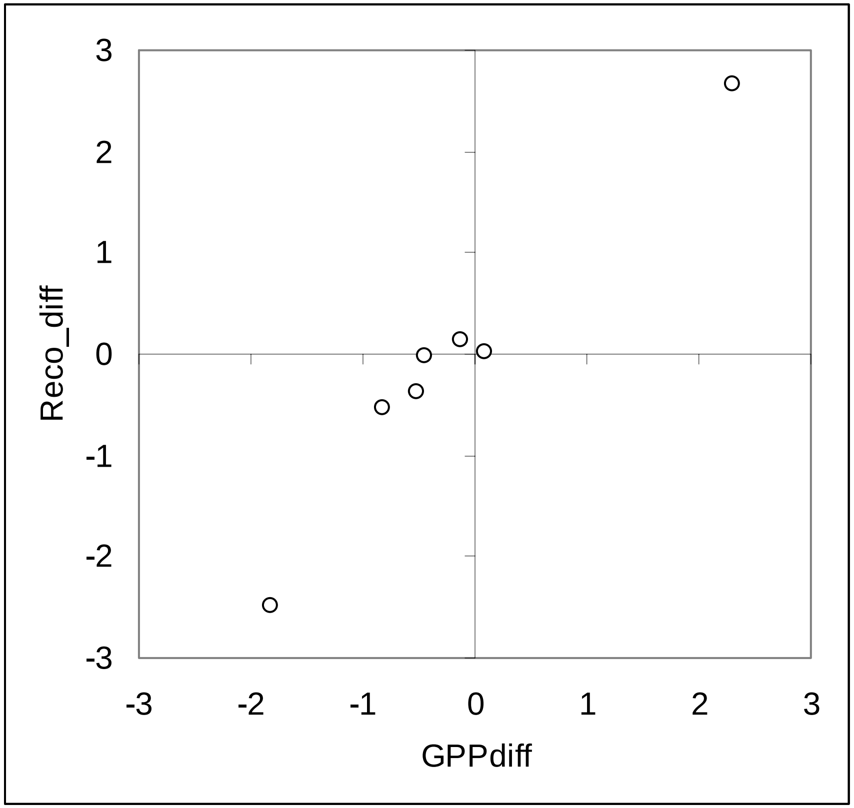

2003 modelling system

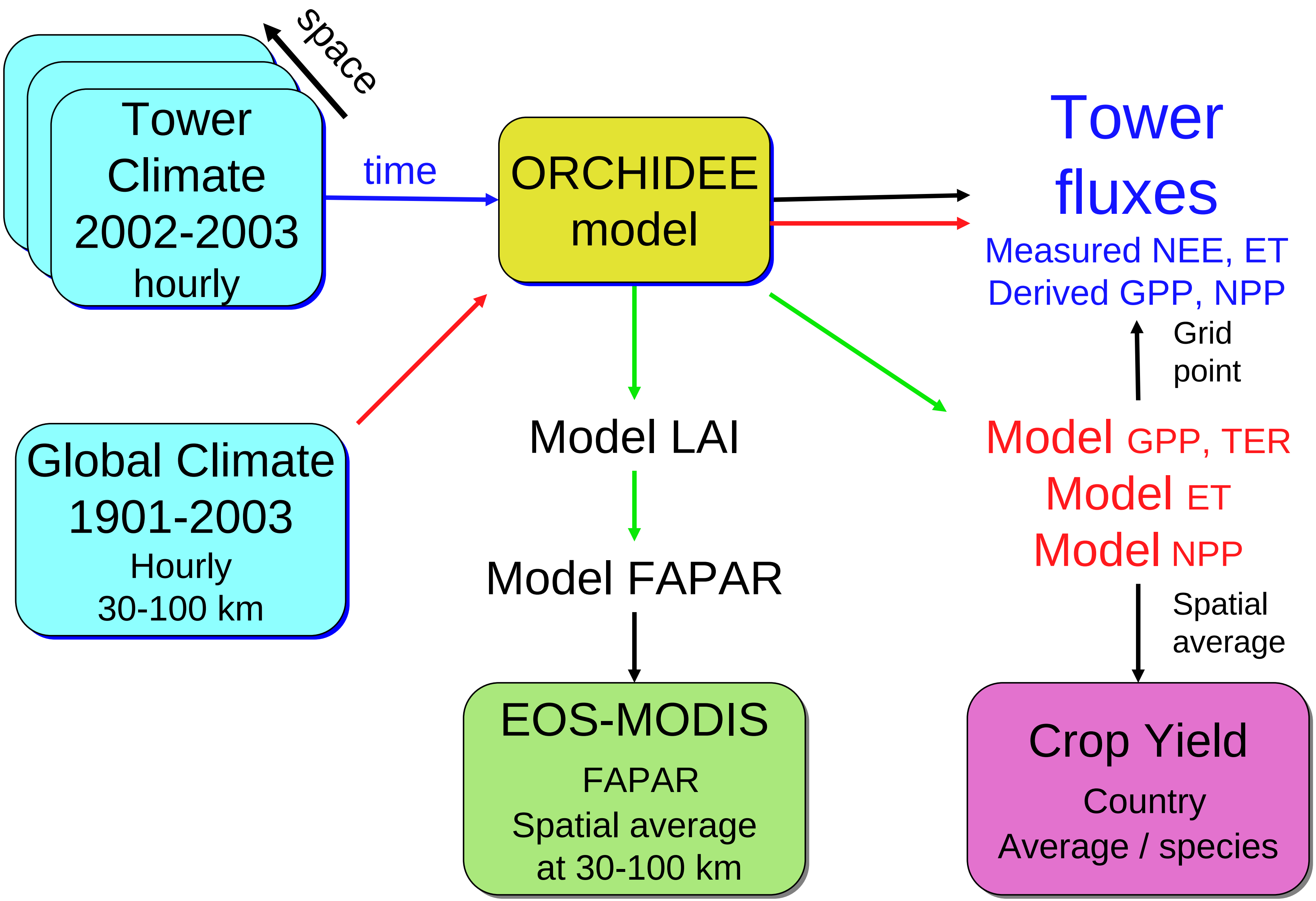

Global biospheric model ORCHIDEE

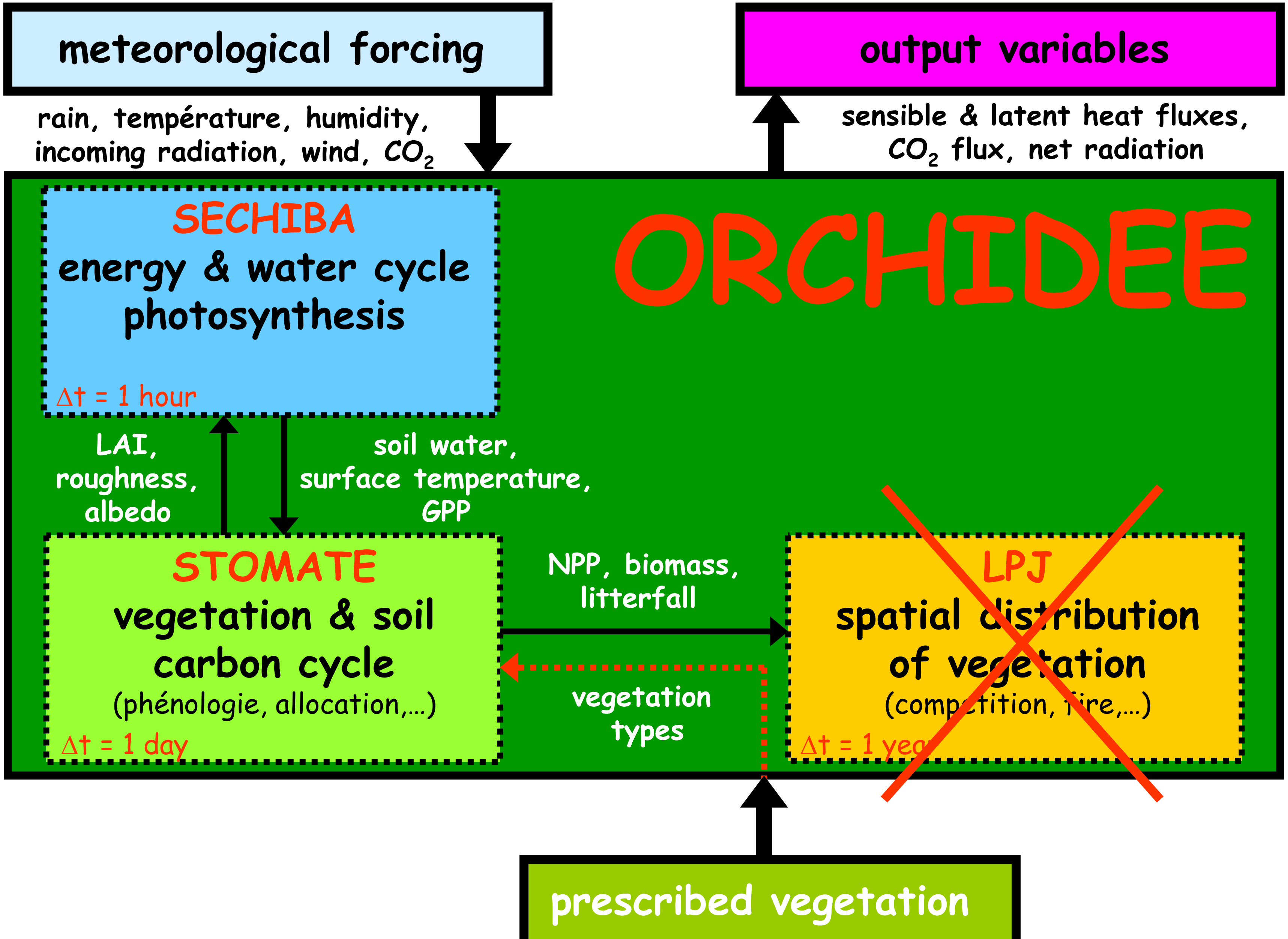

Gross and net fluxes in 2002 and 2003

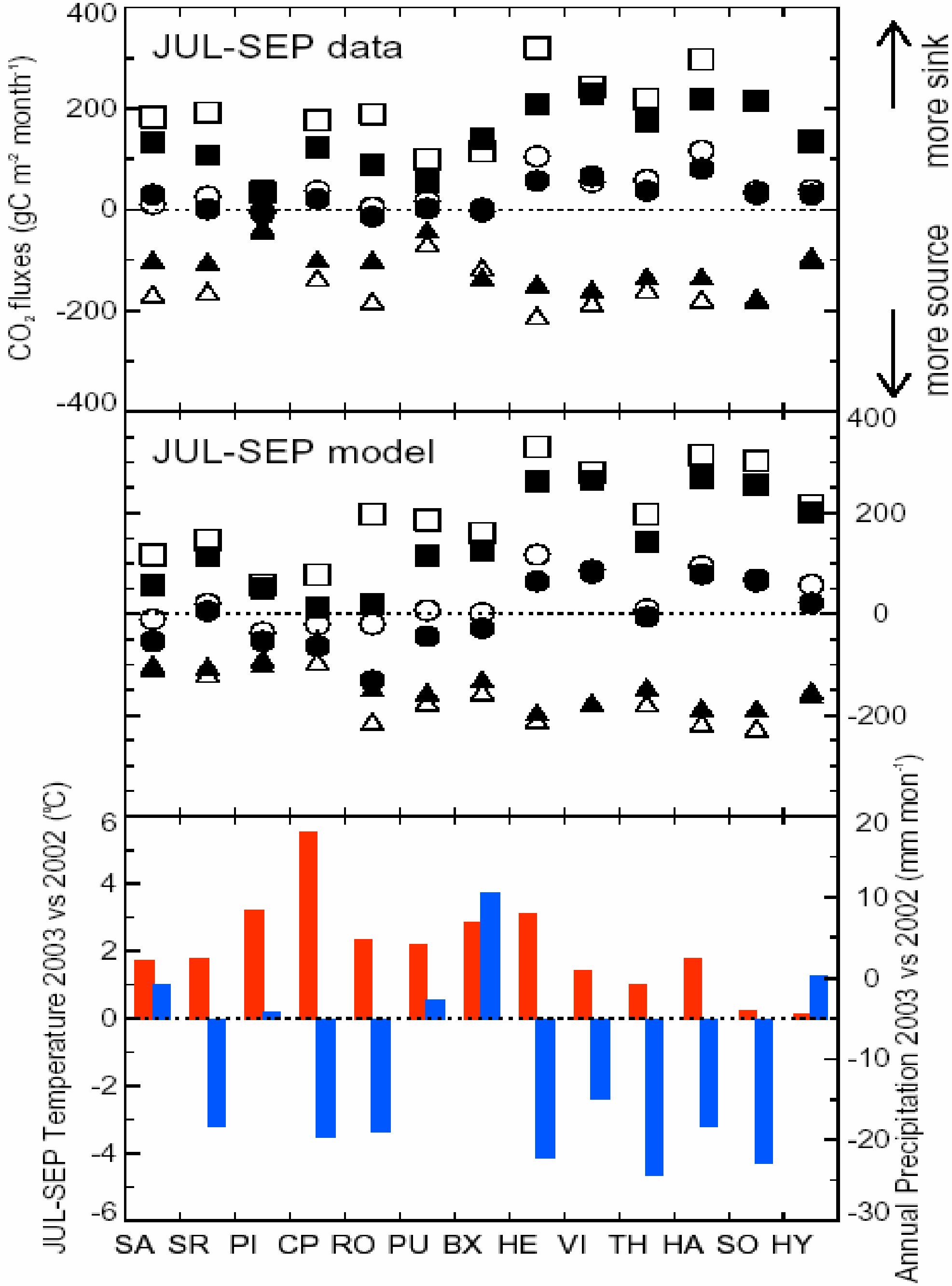

Abnormal Climate and Productivity in 2003

Model verification with EOS-MODIS FAPAR

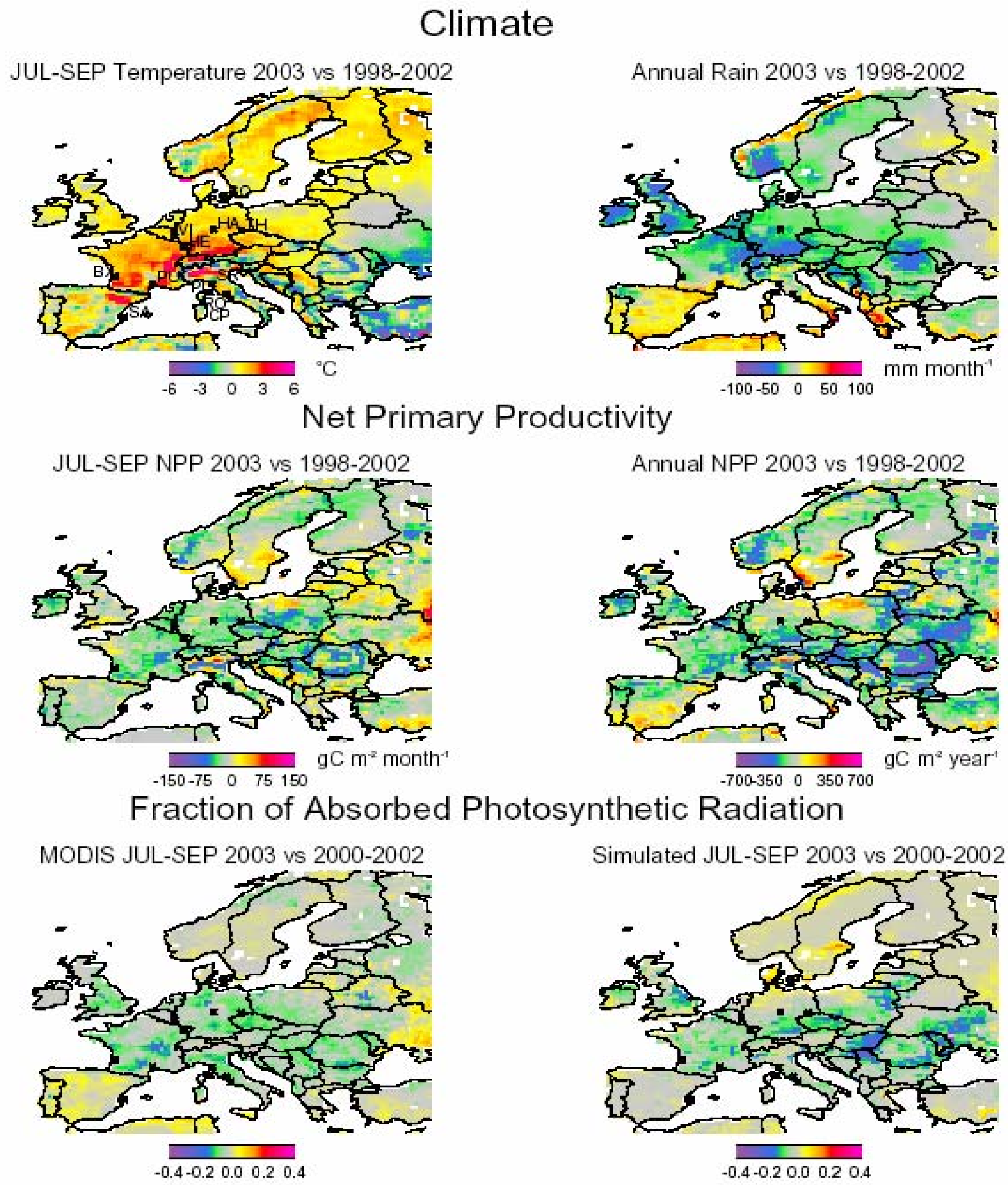

Verification against crops yield national data

QuickTime™ et un
décompresseur TIFF (LZW)
sont requis pour visionner cette image.

2003 is the largest productivity crash of the past 100 years

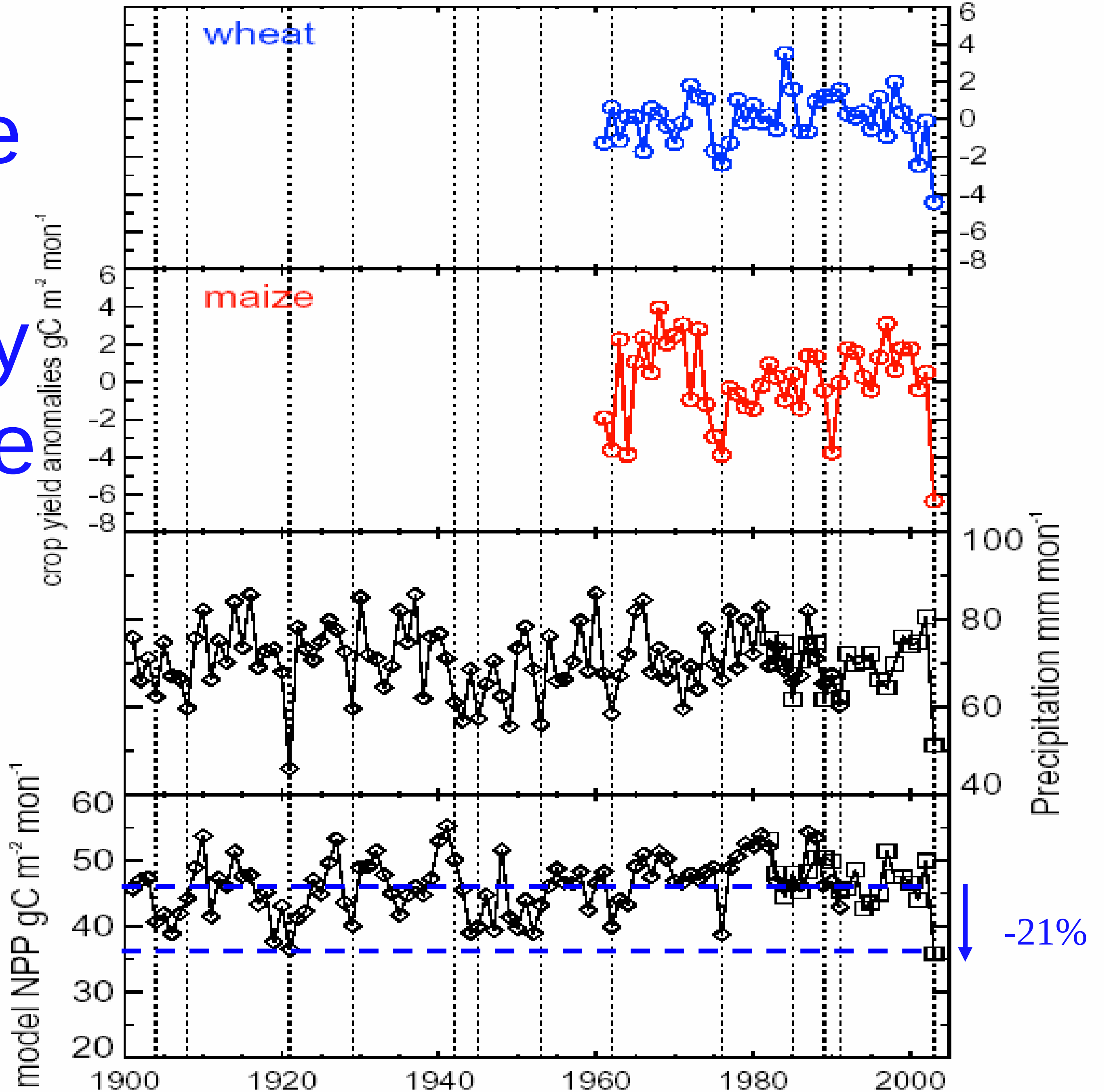

Independent tree ring verification

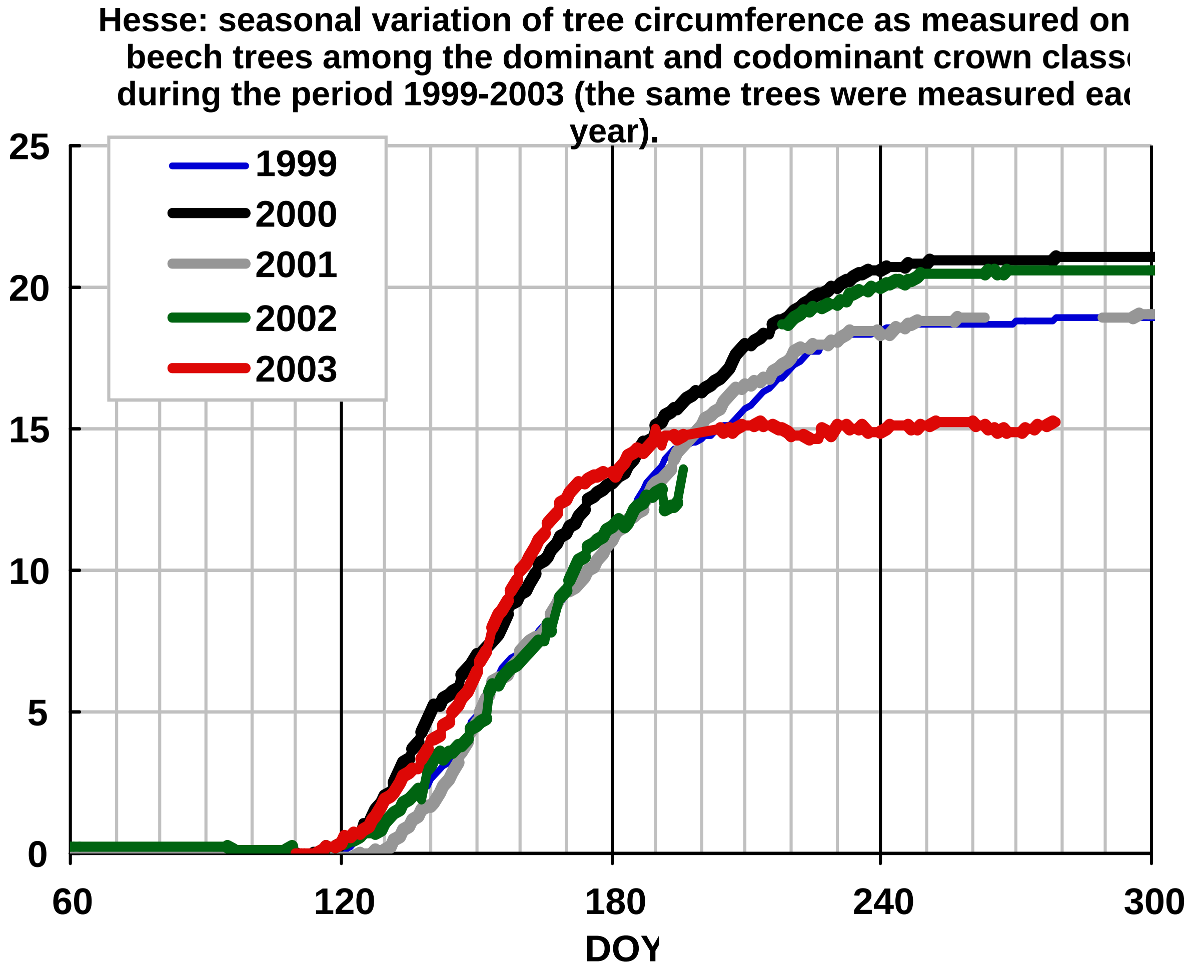

A. Granier pers. Comm

Independent Atmospheric Verification of NEE (in progress)

Monte cimone, 2100 m (Italy)

Schauinsland, 1200 m (Germany)

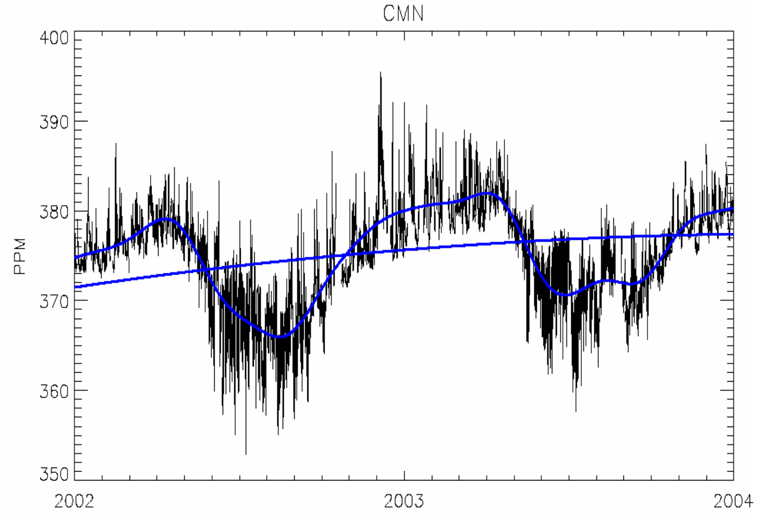

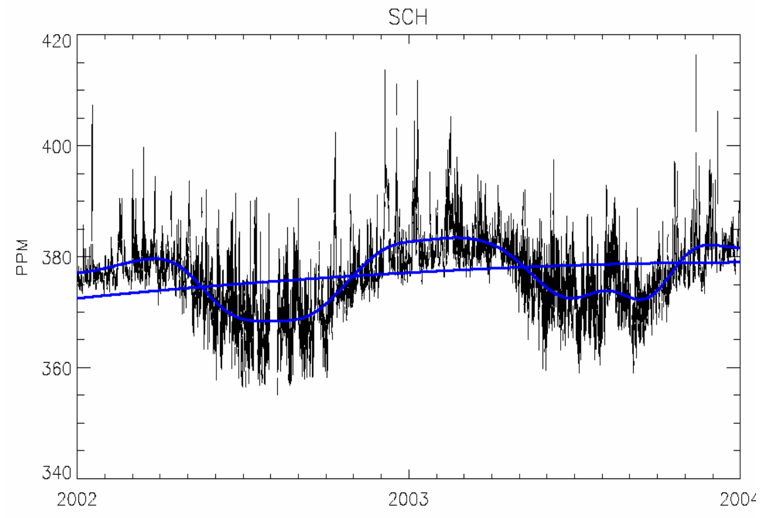

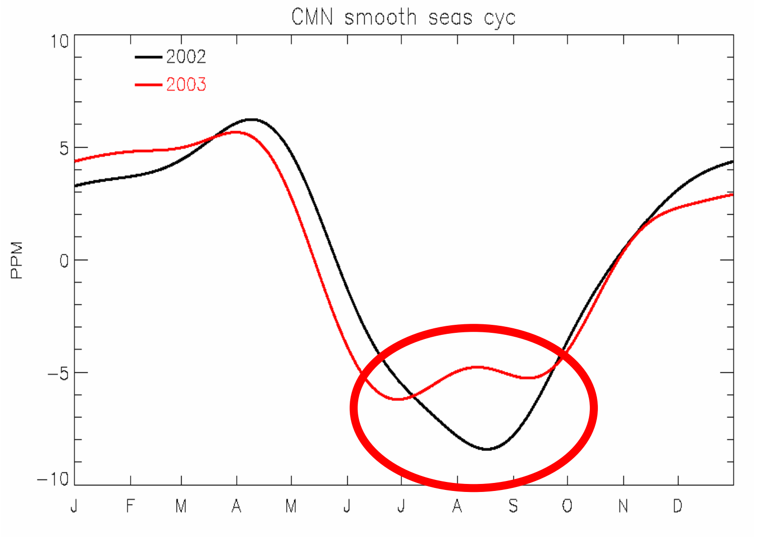

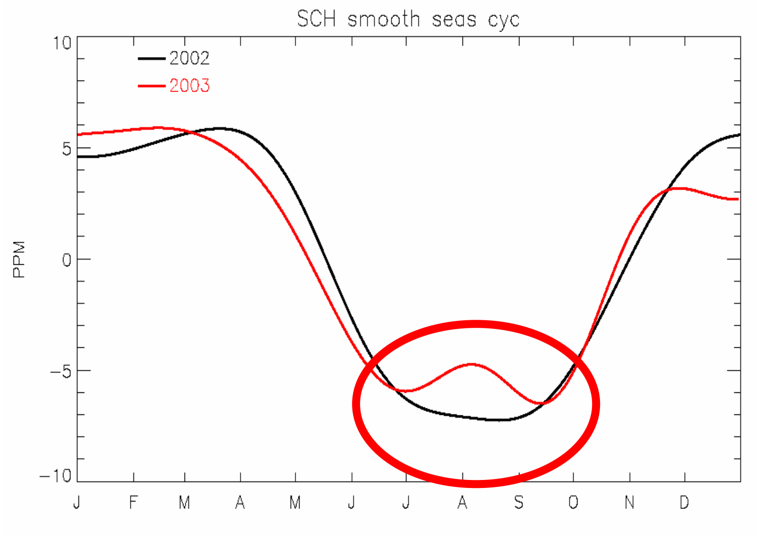

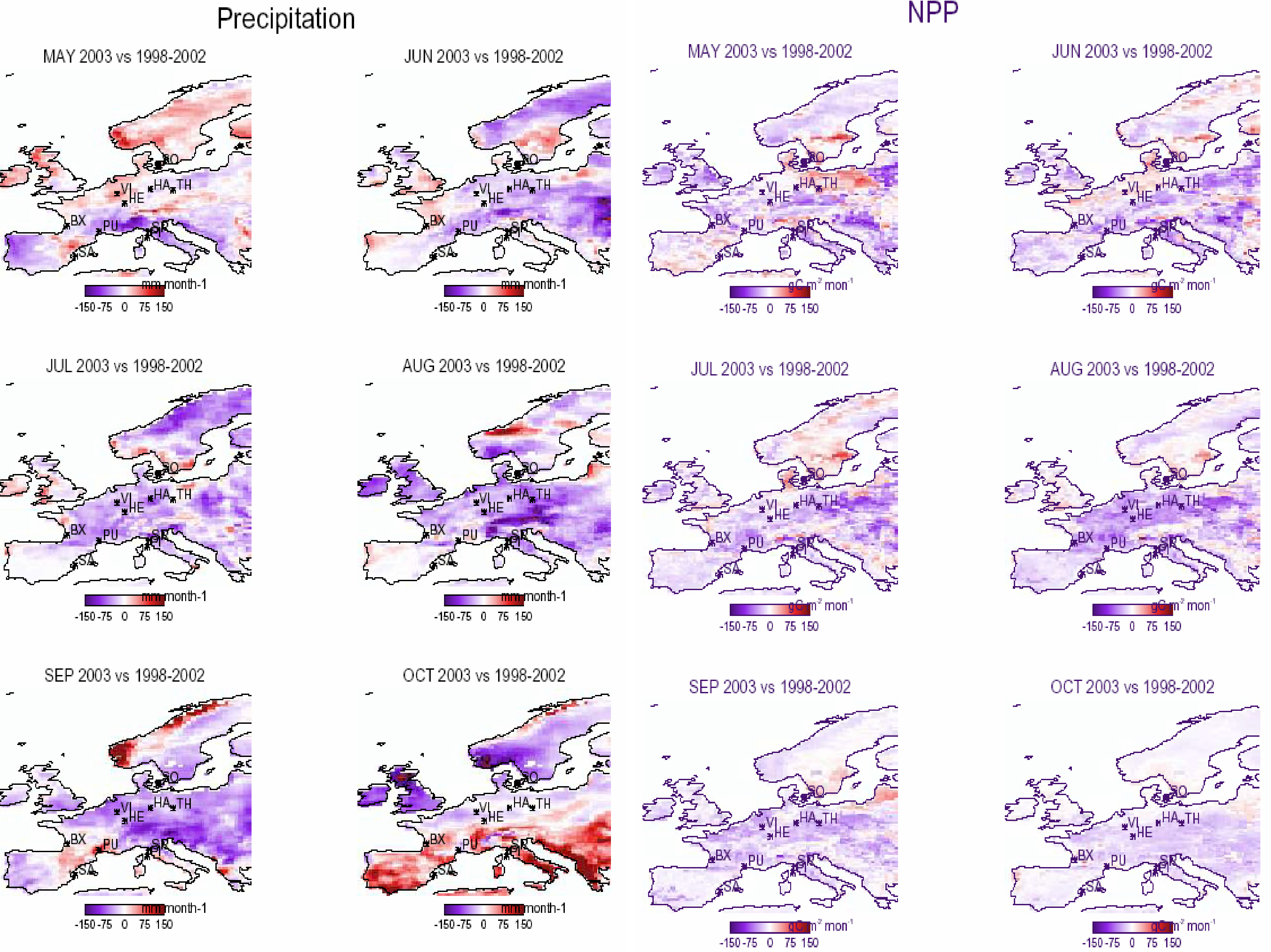

Precipitation
NPP
MAY 2003 vs 1998-2002
JUN 2003 vs 1998-2002
JUL 2003 vs 1998-2002
AUG 2003 vs 1998-2002
SEP 2003 vs 1998-2002
OCT 2003 vs 1998-2002
SO
VI
HE
HA
TH
BX
PU
SR
SA
mm month-1
gC m^{-2} mon^{-1}
-150 -75 0 75 150

Did Rainfall deficit drives the GPP decrease ?

Model

QuickTime™ et un
décompresseur TIFF (LZW)
sont requis pour visionner cette image.

Flux towers

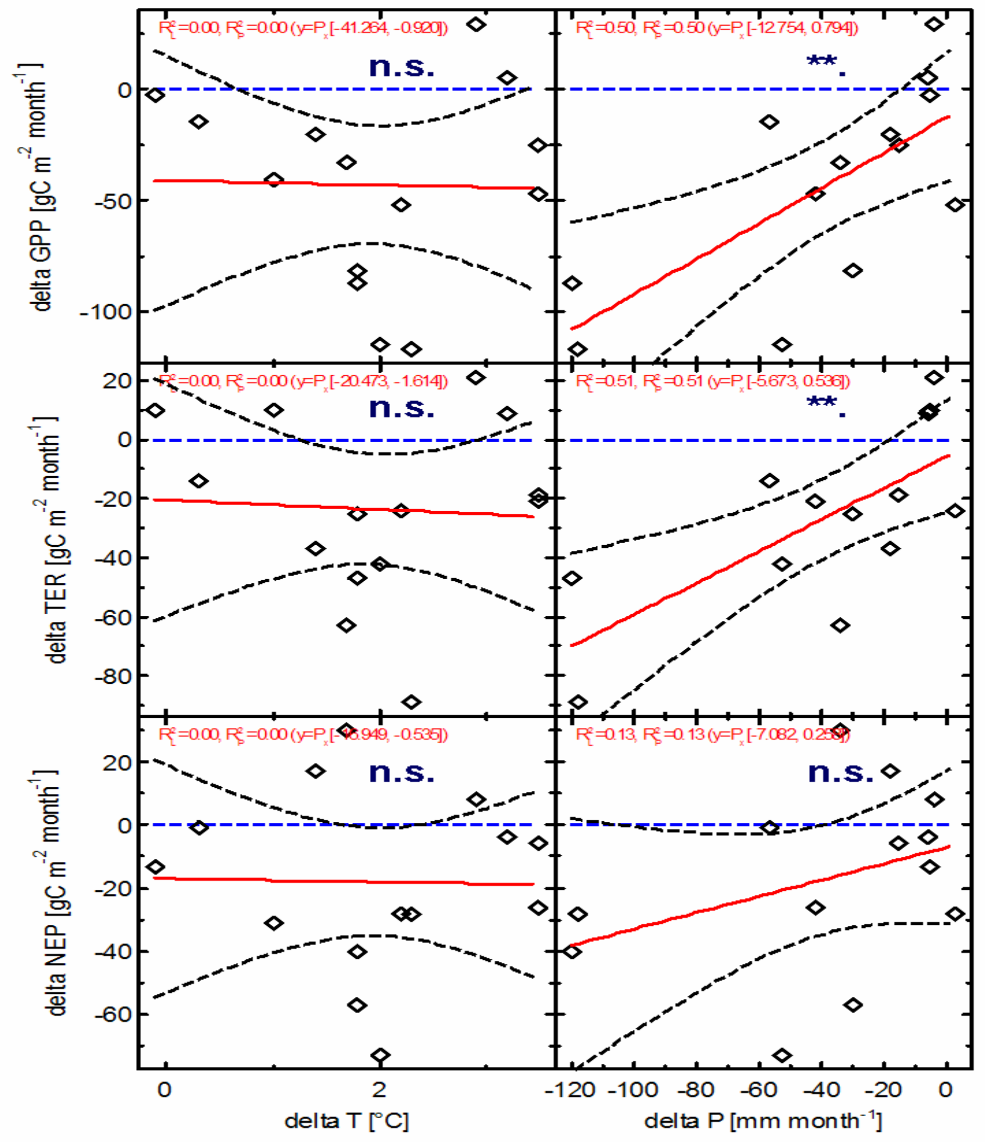

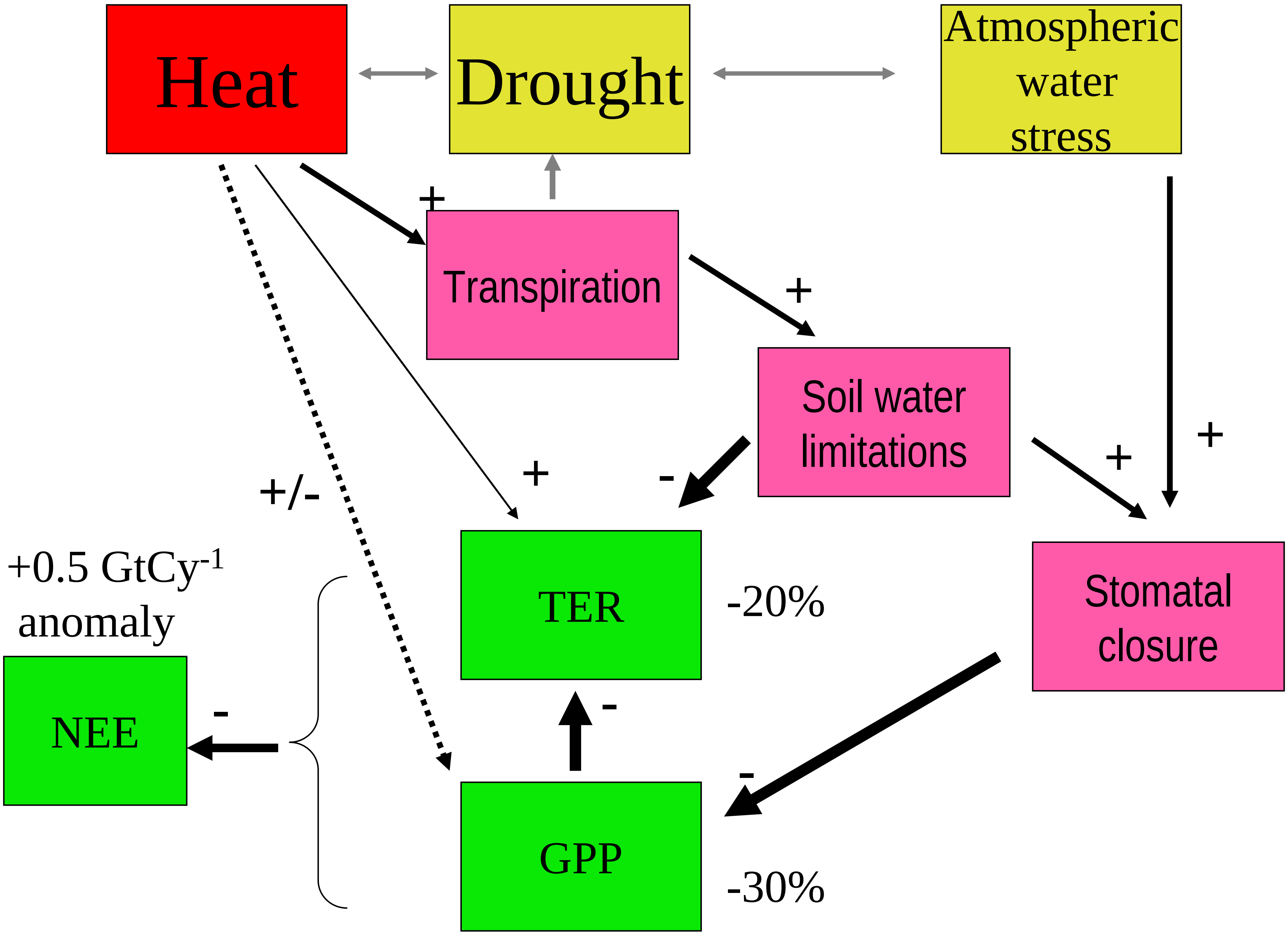

Heat
Drought
Atmospheric water stress
+
Transpiration
+
Soil water limitations
+
+
+
-
+
+/-
+0.5 GtCy-1 anomaly
TER
-20%
Stomatal closure
NEE
-
-
-
GPP
-30%

Soil water content variation model and observations indicate large water stress at all sites in 2003 with Root Extractable Water (REW) < 0.4

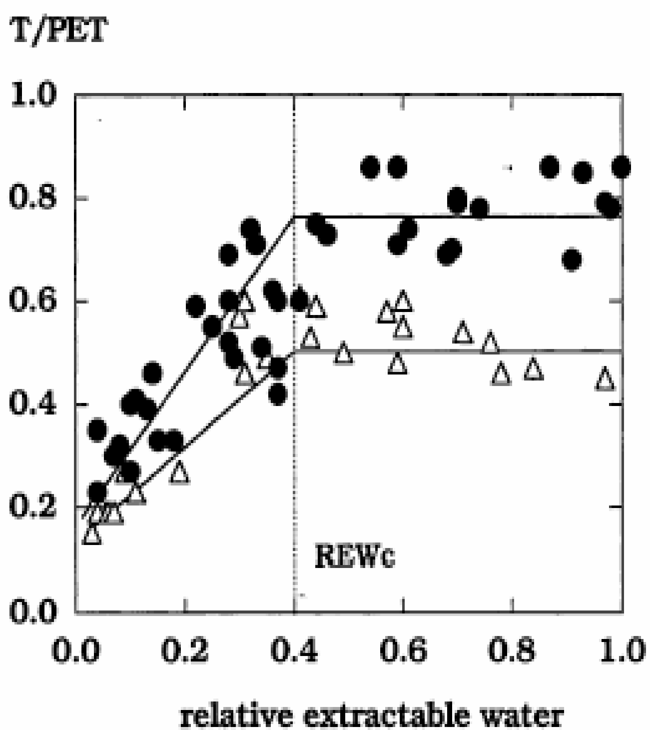

Fig. 2. Ratio T/PET calculated from sap flow measurements in an oak stand as a function of relative extractable water (REW) calculated from neutron probe measurements (from Bréda and Granier, 1996). Two data sets are reported: LAI = 6 m^2 m^{-2} (black circles) and LAI = 4.5 m^2 m^{-2} (open triangles). The dotted line shows the critical REW (REW_c).

Breda et al. 1999

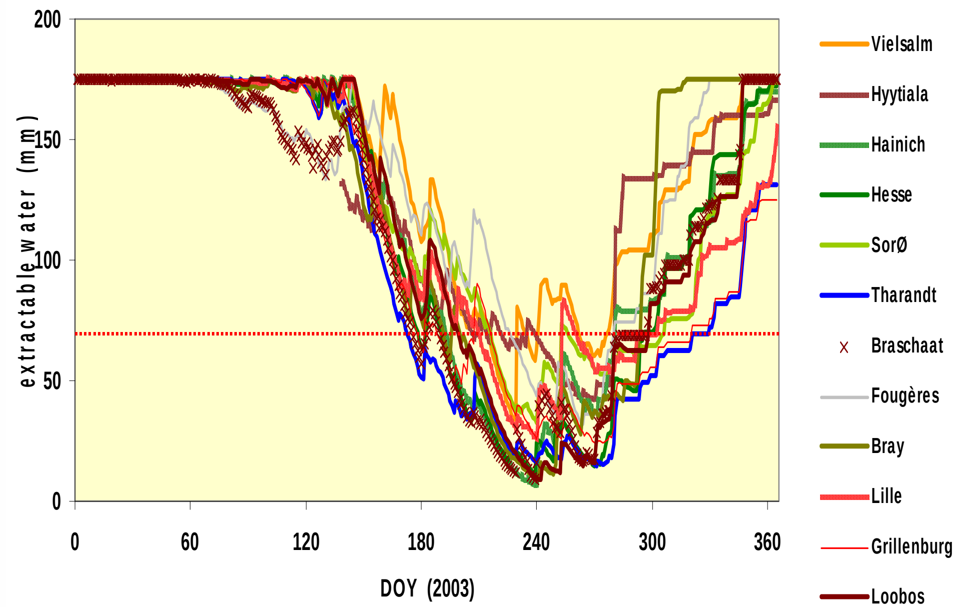

Granier et al. analysis confirms water-stress controls

Canopy conductance correlates with soil water stress

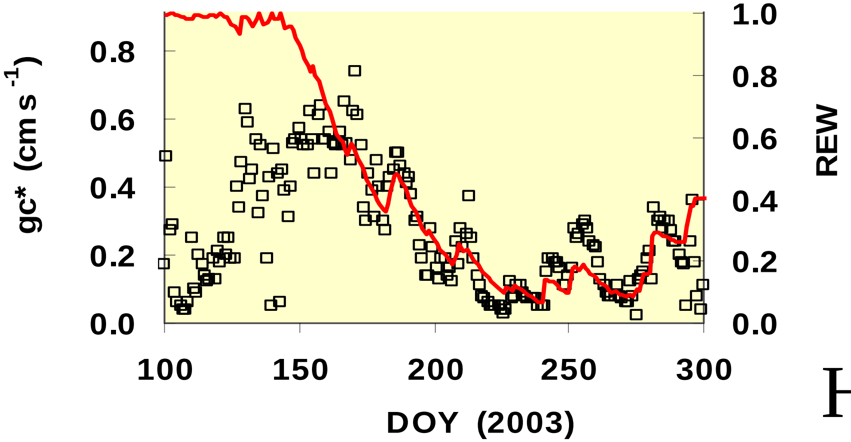

Canopy conductance in 2003 at Hesse was 15% of its 2002 value !

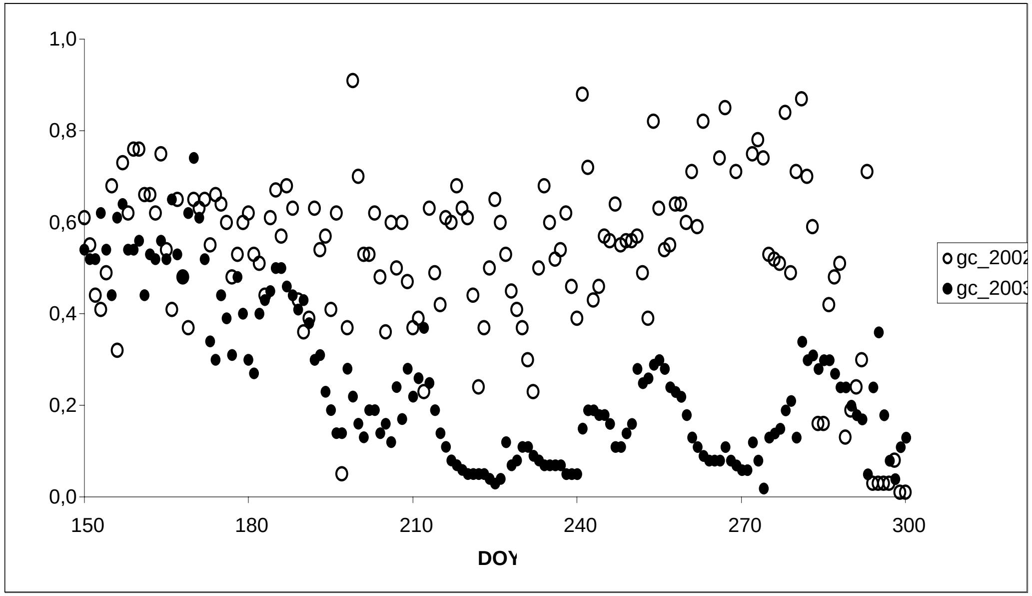

Modellers, be brave !
test your best parameters for 2003!

See also Wang et al. , Poster by Santaren, etc..

BIOME-BGC Model Parameters

Deciduous broadleaf forest

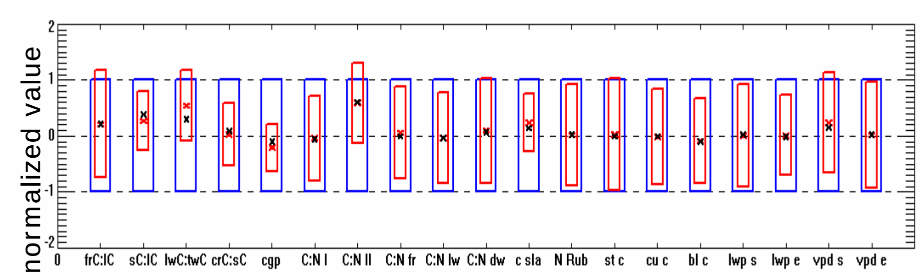

Evergreen needle leaf forest

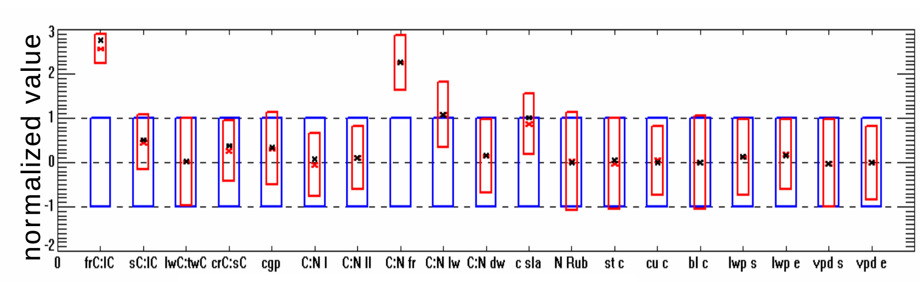

ecophysiological parameters

Parameter range before optimization

Parameter range after optimization

Model Results

NEE

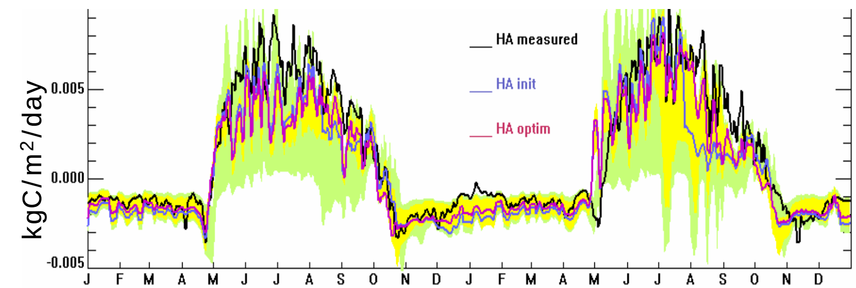

Leaf Area Index

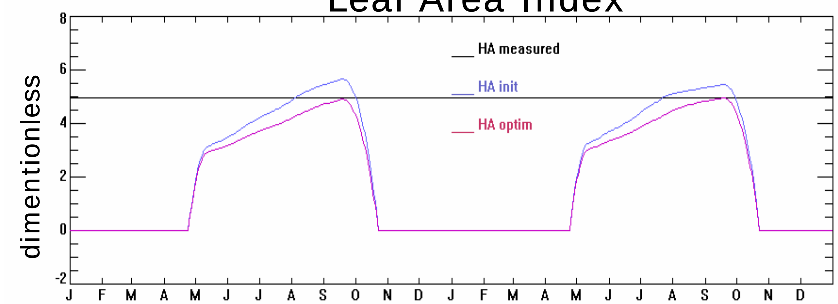

month

Trusilova and Churkina
in preparation

Joint constraints! Complementary methods 3. Regional Inversions

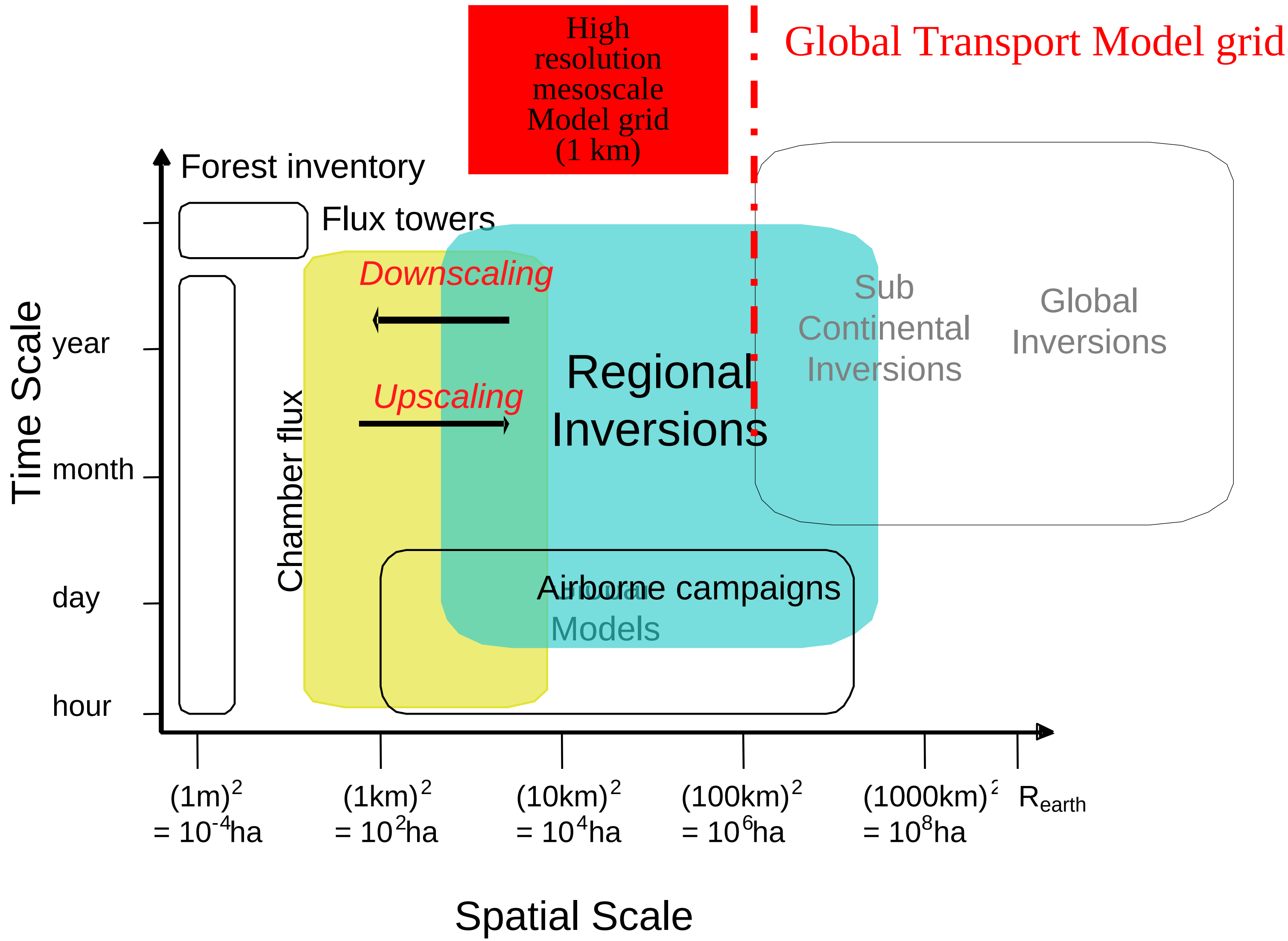

WLEF CO_2 flux and mixing ratio observatory
K. Davis and colleagues

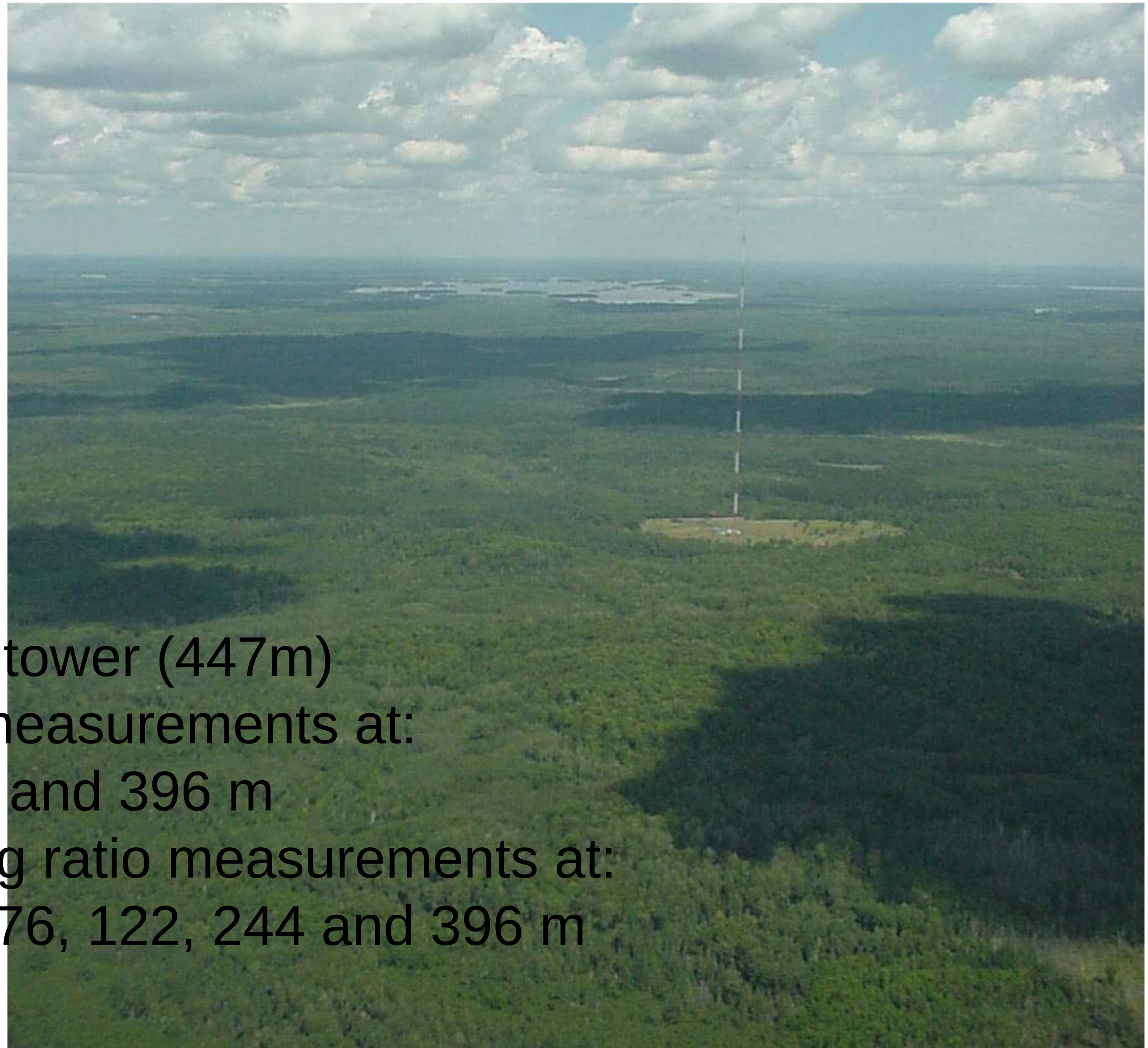

WLEF tall tower (447m)

CO_2 flux measurements at:

30, 122 and 396 m

CO_2 mixing ratio measurements at:

11, 30, 76, 122, 244 and 396 m

Photo credit: UND Citation crew, COBRA

ChEAS Regional Flux Experiment Domain

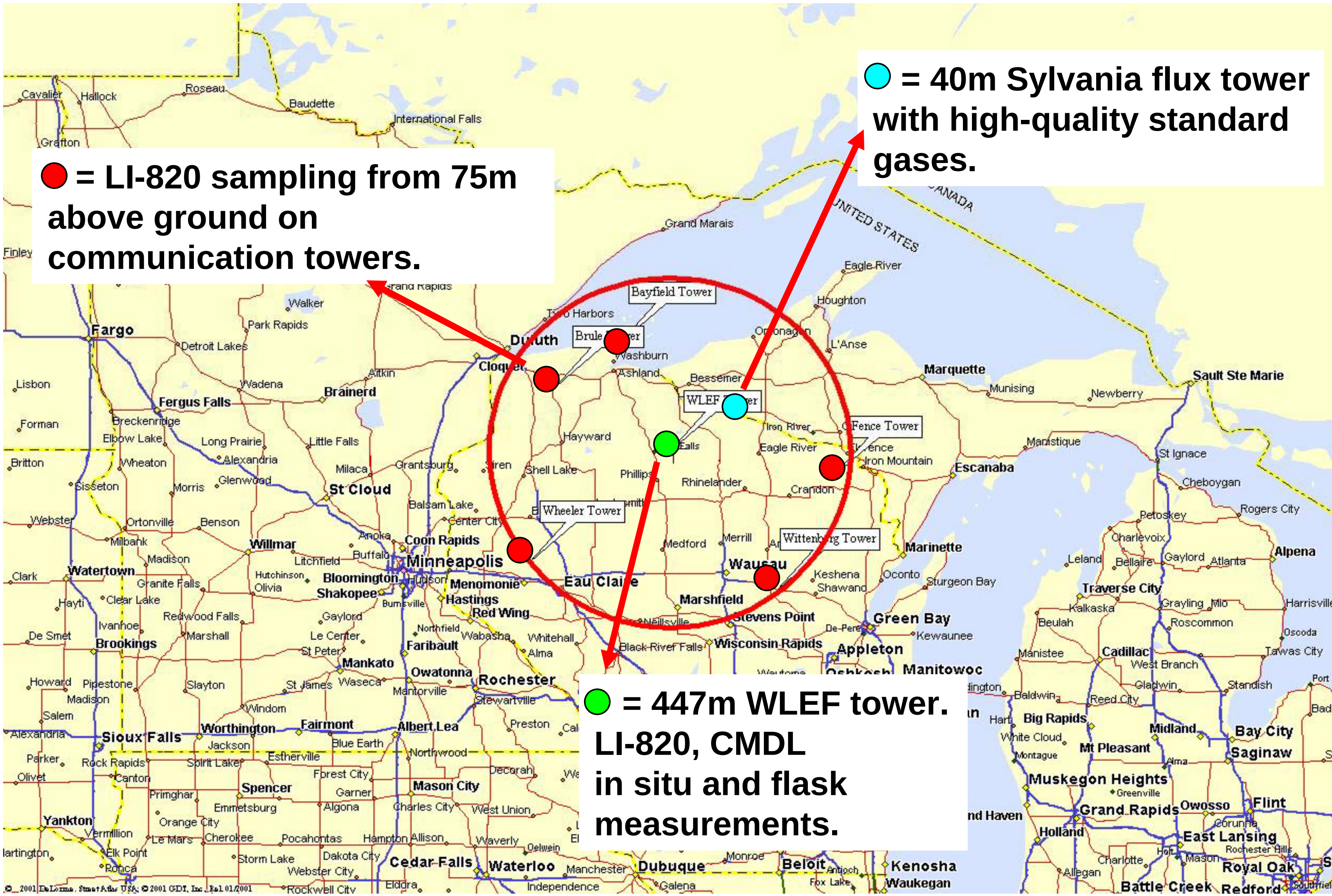

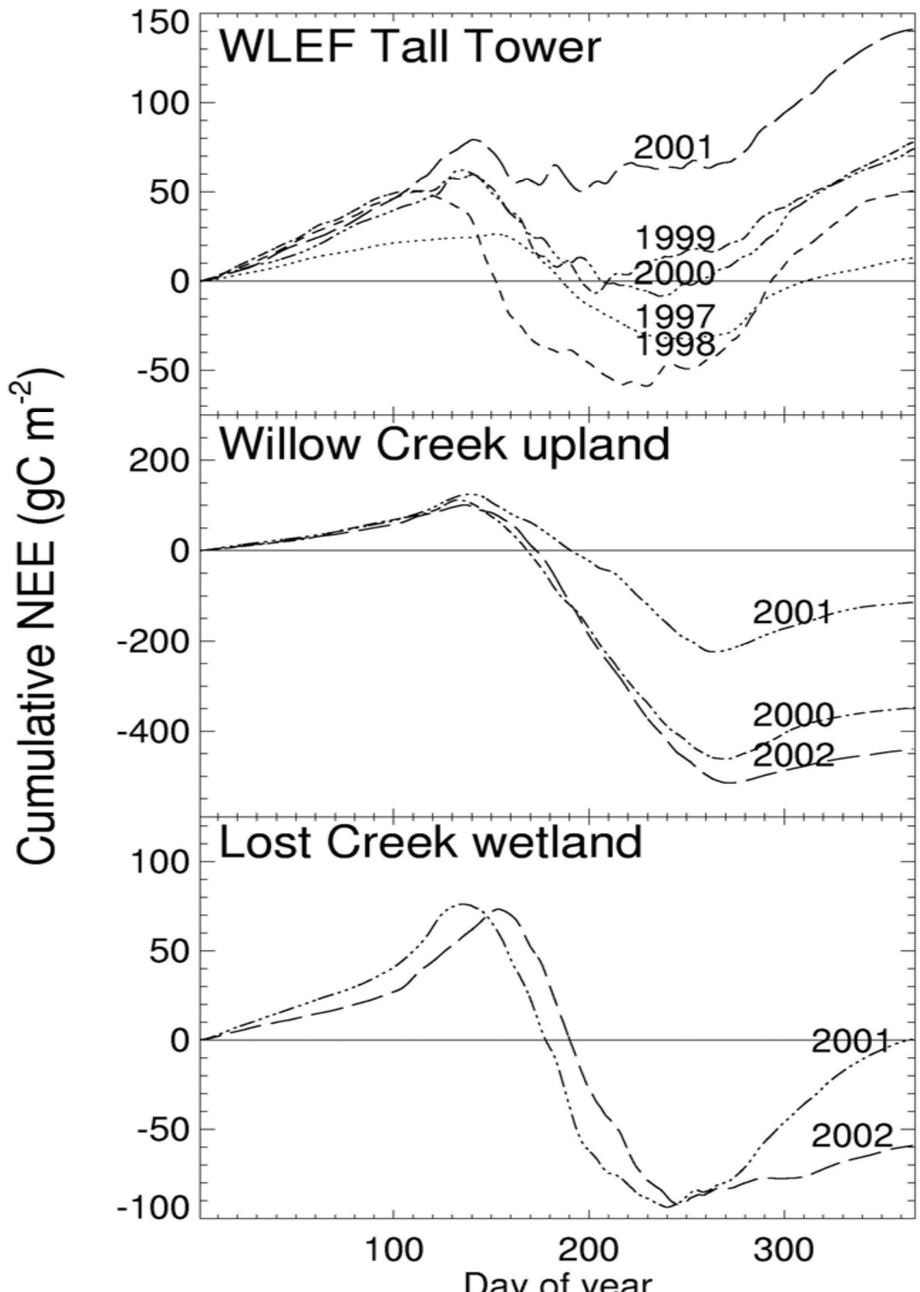
WLEF Tall Tower
Willow Creek upland
Lost Creek wetland
Cumulative NEE (gC m-2)
Day of year
2001
1999
2000
1997
1998
2002
150
100
50
0
-50
200
-200
-400
-100
300

NEE and gross fluxes at ChEAS sites: 1997-2002

	NEE ($gC\ m^{-2}$)	Respiration ($gC\ m^{-2}$)	Photosynthesis ($gC\ m^{-2}$)
WLEF 1997	27	991	964
WLEF 1998	48	986	938
WLEF 1999	100	1054	954
WLEF 2000	74	1005	931
WLEF 2001	141	1067	926
WLEF average	**78**	**1021**	**942**
Willow Creek 2000	-347	762	1109
Willow Creek 2001	-108	741	849
Willow Creek 2002	-437	648	1085
Willow Creek average	**-297**	**717**	**1014**
Lost creek 2001	1	759	758
Lost Creek 2002	-58	631	689
Lost Creek average	**-30**	**695**	**724**

ChEAS Regional Flux Experiment

- Derive daytime and daily seasonal fluxes using regional atmospheric inversions and relatively inexpensive in situ CO_2 sensors.
- Overarching goal – evaluate/merge multiple approaches of studying terrestrial fluxes of CO_2.
  - Merge flux-tower based upscaling with downscaled inversion methodology. Regional integration and mechanistic interpretation.
  - Determine interannual variations in seasonal fluxes on a regional basis. Again, integrate with regional flux measurements/mechanistic interpretations.
  - If possible, derive net annual fluxes. Spatial resolution is limited by the magnitude of the annual signal.

Expected Regional Mixing Ratio Differences (Winter to Summer)

Time scale	Daytime	Diurnal	Annual
Flux magnitude	1 to 10 μmol m^{-2} s^{-1}	1 to 4 gC m^{-2} d^{-1}	~ 1 gC m^{-2} d^{-1}
Mixing depth	1 to 2 km	1 to 2 km	~10 km
Advection time	~10 hours	~24 hours	
Advection distance	~180 km (half ring)	~400 km (full ring)	400 km (full ring)
Change in ABL CO_2	1 to 5 ppm	2 to 5 ppm	~0.2 ppm

Climatology of influence functions for August 2000

- influence functions derived from RAMS/LPD model simulations
- passive tracer
- different configurations of concentration samples - time series from
  - a single level of WLEF tower
  - all levels of WLEF tower
  - six additional towers

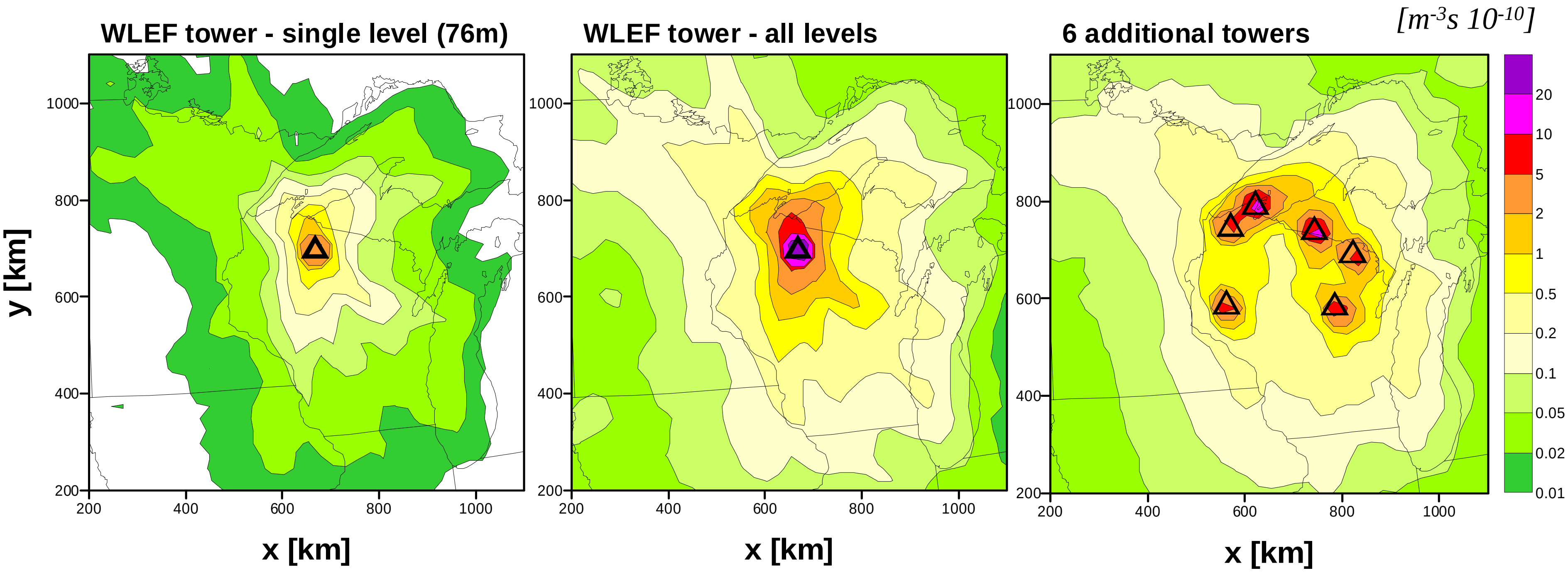

Regional Inversions

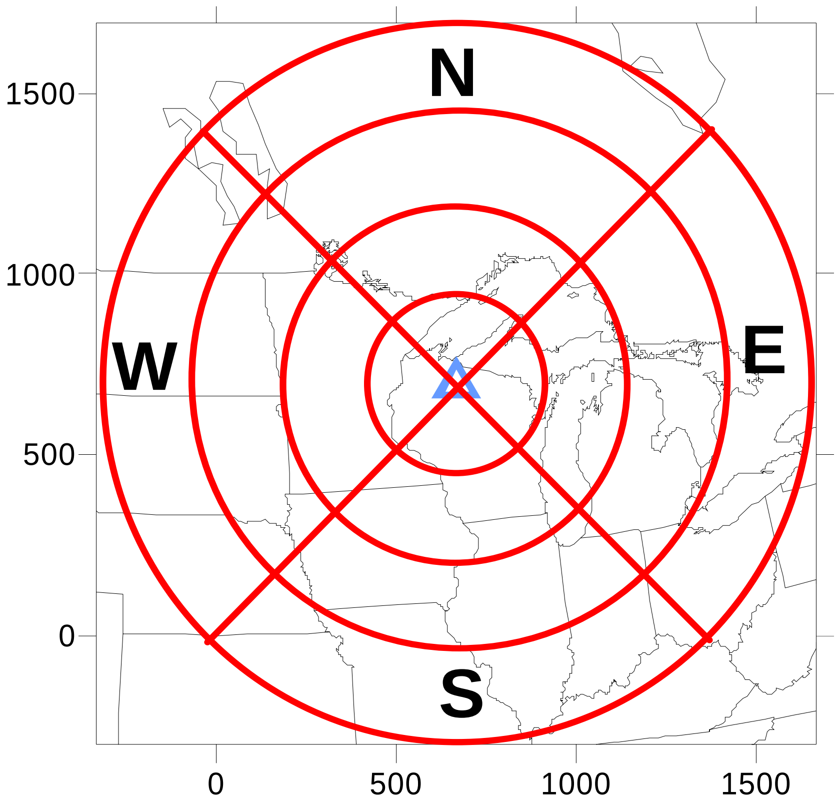

Separate estimation of A(PAR), R(T), FF

- Bayesian inversion technique
- source areas defined in polar coordinates centered at the WLEF tower
  - a better coverage by atmospheric transport
- [RAMS -> LPD] long term simulations
  - derivation of influence functions for concentration samples
- data: concentration time series from the WLEF tower and additional towers
- CO_2 flux decomposed into respiration and assimilation fluxes
- CO_2 inflow fluxes from a larger scale model
  - a priori estimations to be improved in inversion calculations

Example of estimation of NEE averaged for August 2000

✓ Inversion calculations for increasing number of concentration data (time series from towers)

✓NEE uncertainty presented in terms of standard deviation derived from posteriori covariance matrix

✓ Inflow CO_2 flux is assumed to be known from a large scale transport model

Configuration of source areas with WLEF tower in the center of polar coordinates

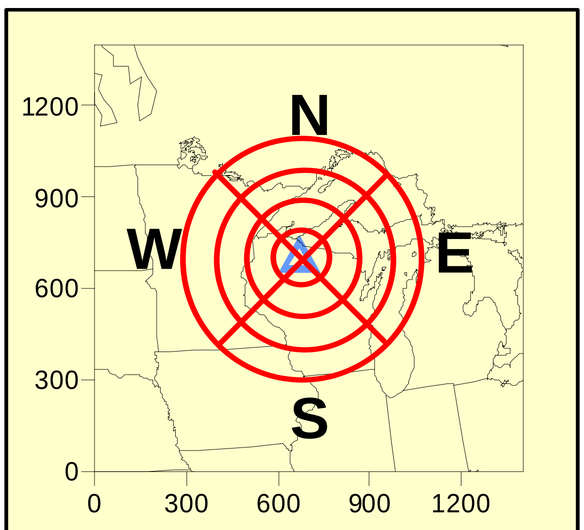

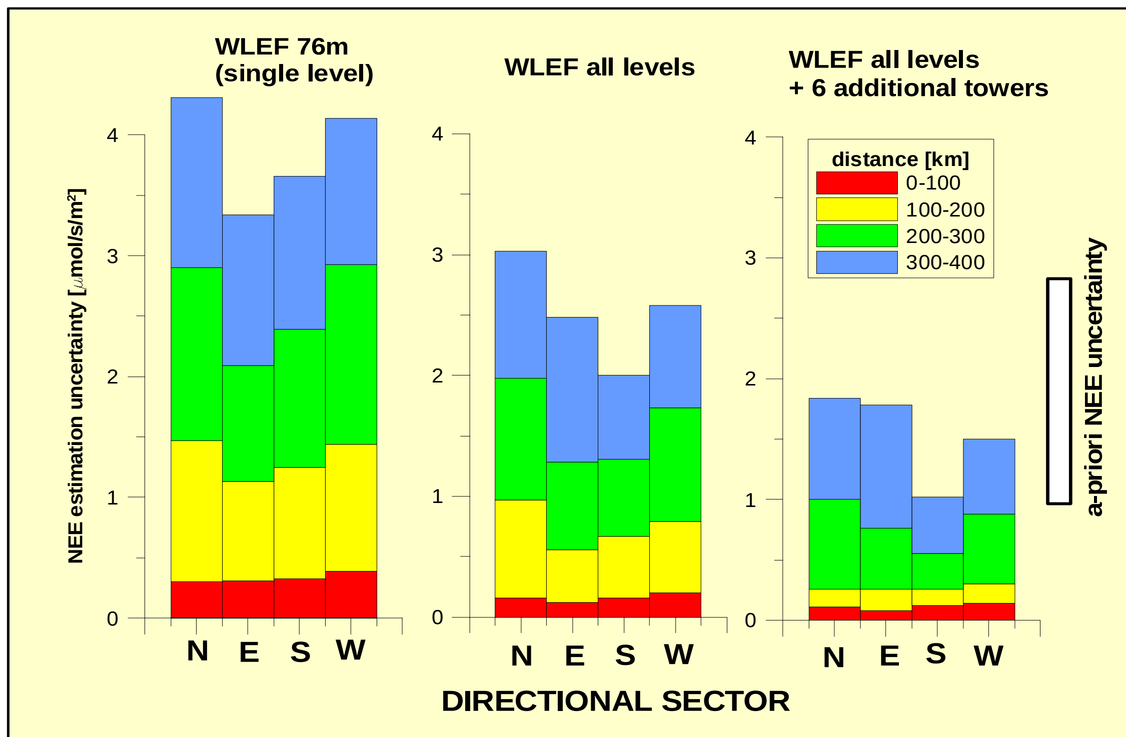

CO2 from 5 sites, April 29, 2004

1200 UTC
April 29, 2004

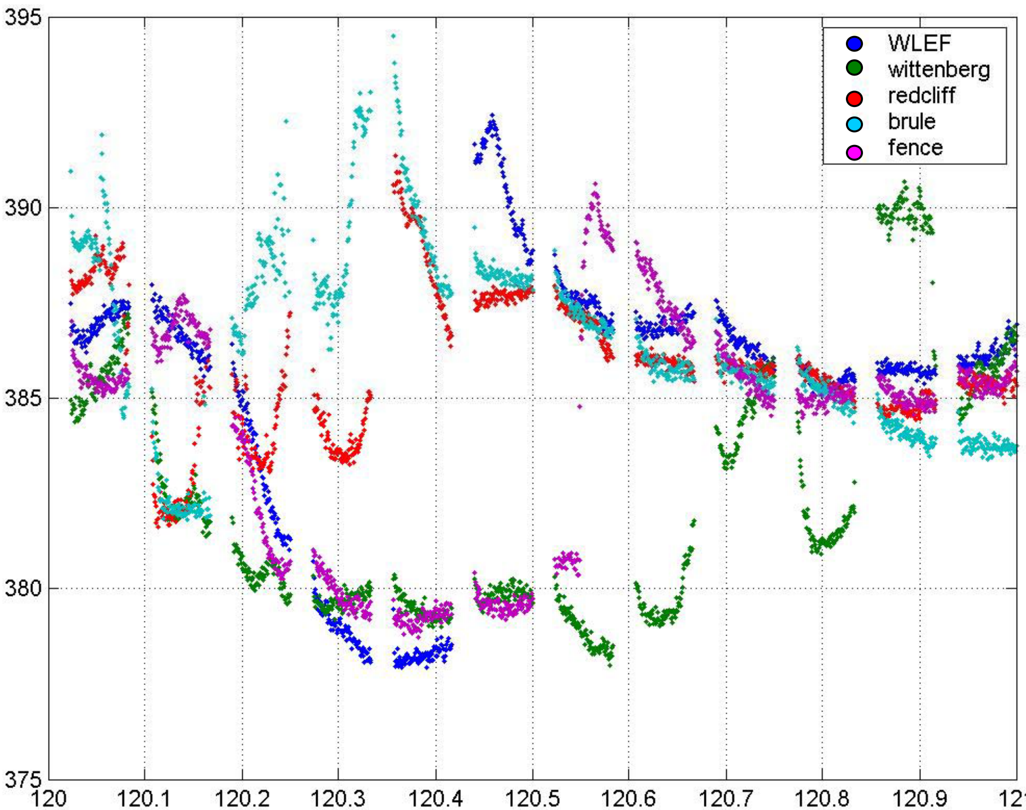

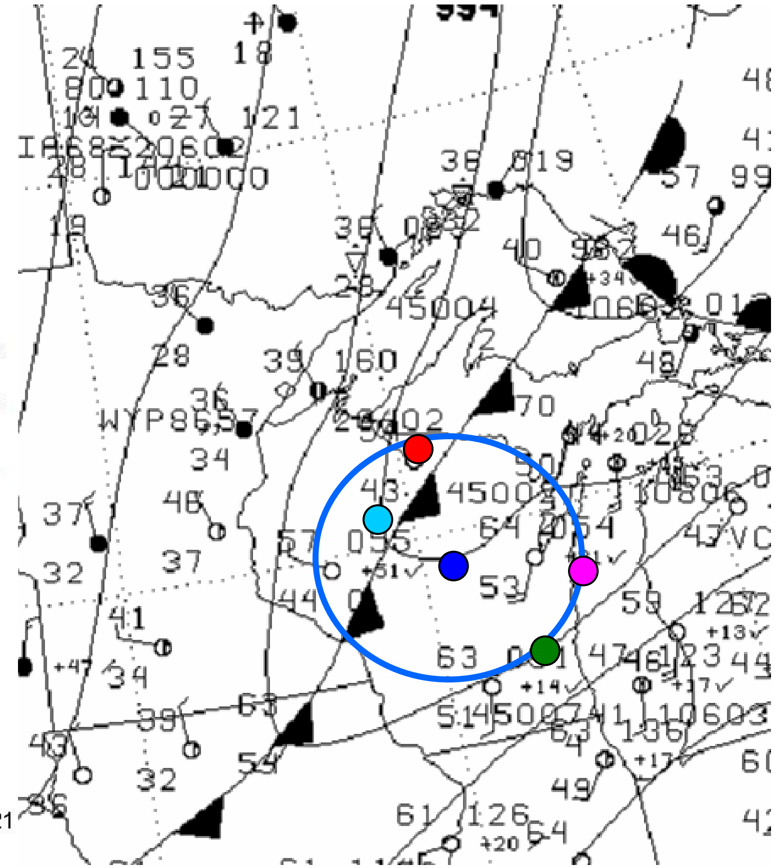

Joint constraints! Complementary methods : Airborne campaigns

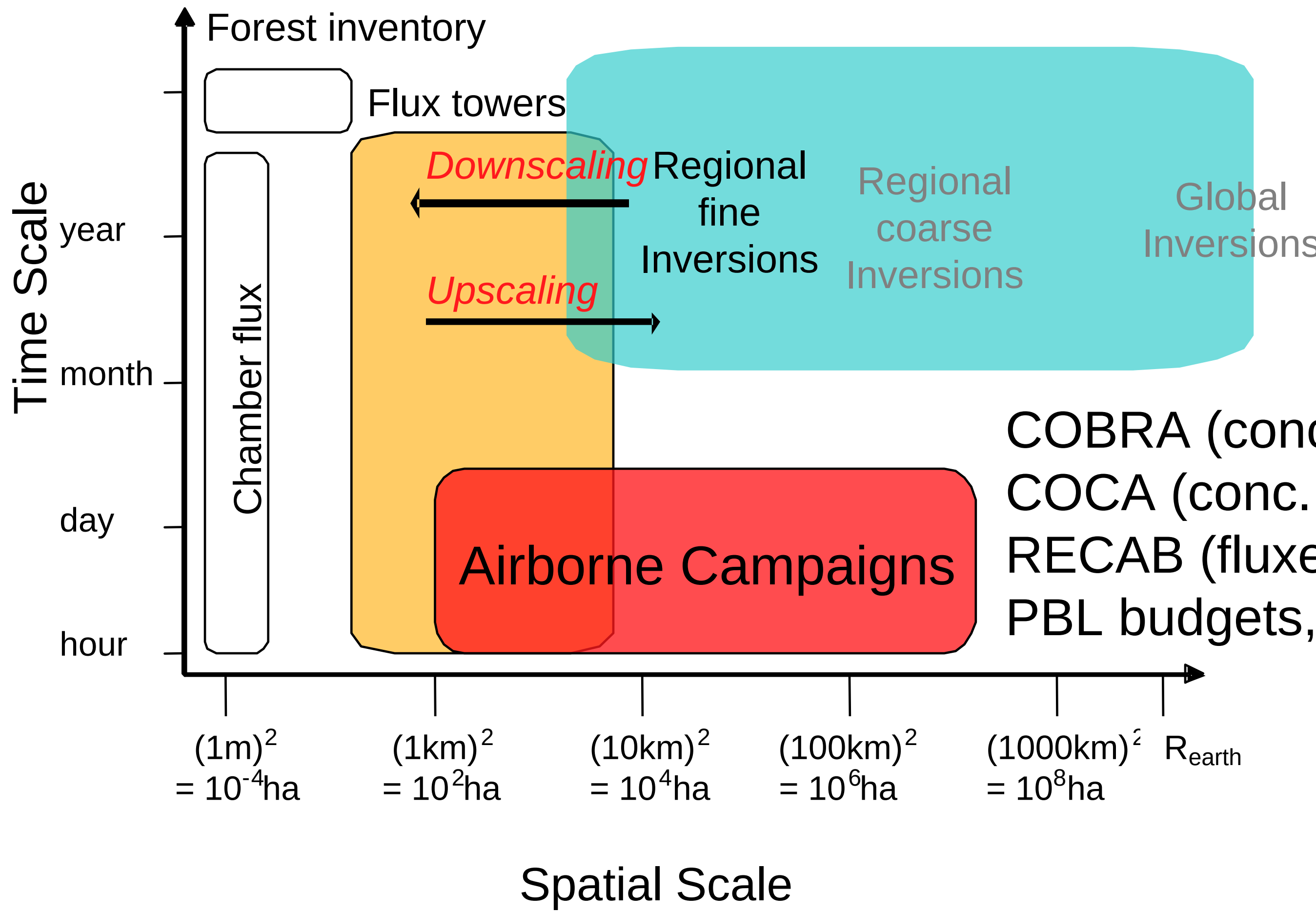

COBRA (concentrations)
COCA (conc. lagrangian)
RECAB (fluxes)
PBL budgets, etc…

Atmospheric and bottom-up regional fluxes in Les landes

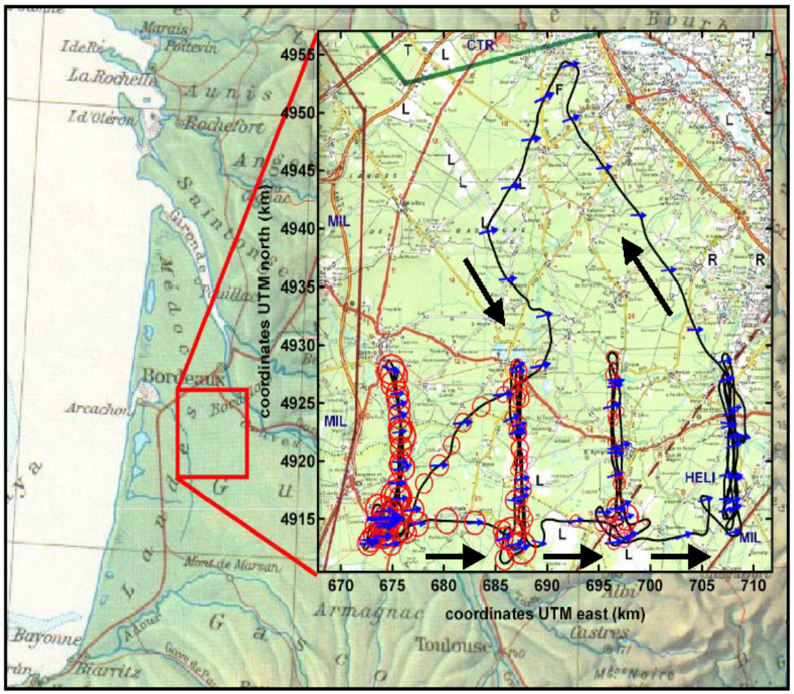

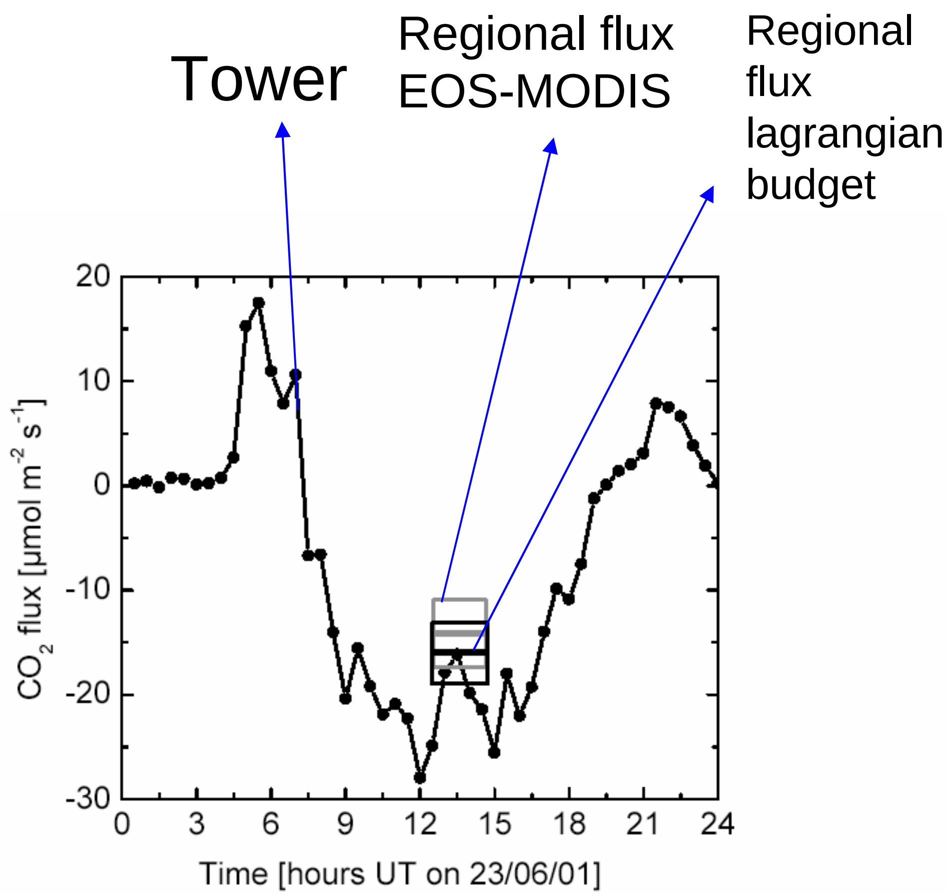

Schmitgen et al. 2004

Figure 7: Net ecosystem CO_2 exchange (NEE) from the eddy correlation measurement at the "Le Bray" tower on 23.06.2001 (circles). The black bar shows the regional NEE from the Lagrangian CBL budget, the gray bar the regional NEE modeled via remote sensing input (the boxes indicate the 1-sigma uncertainties as in Table 4).

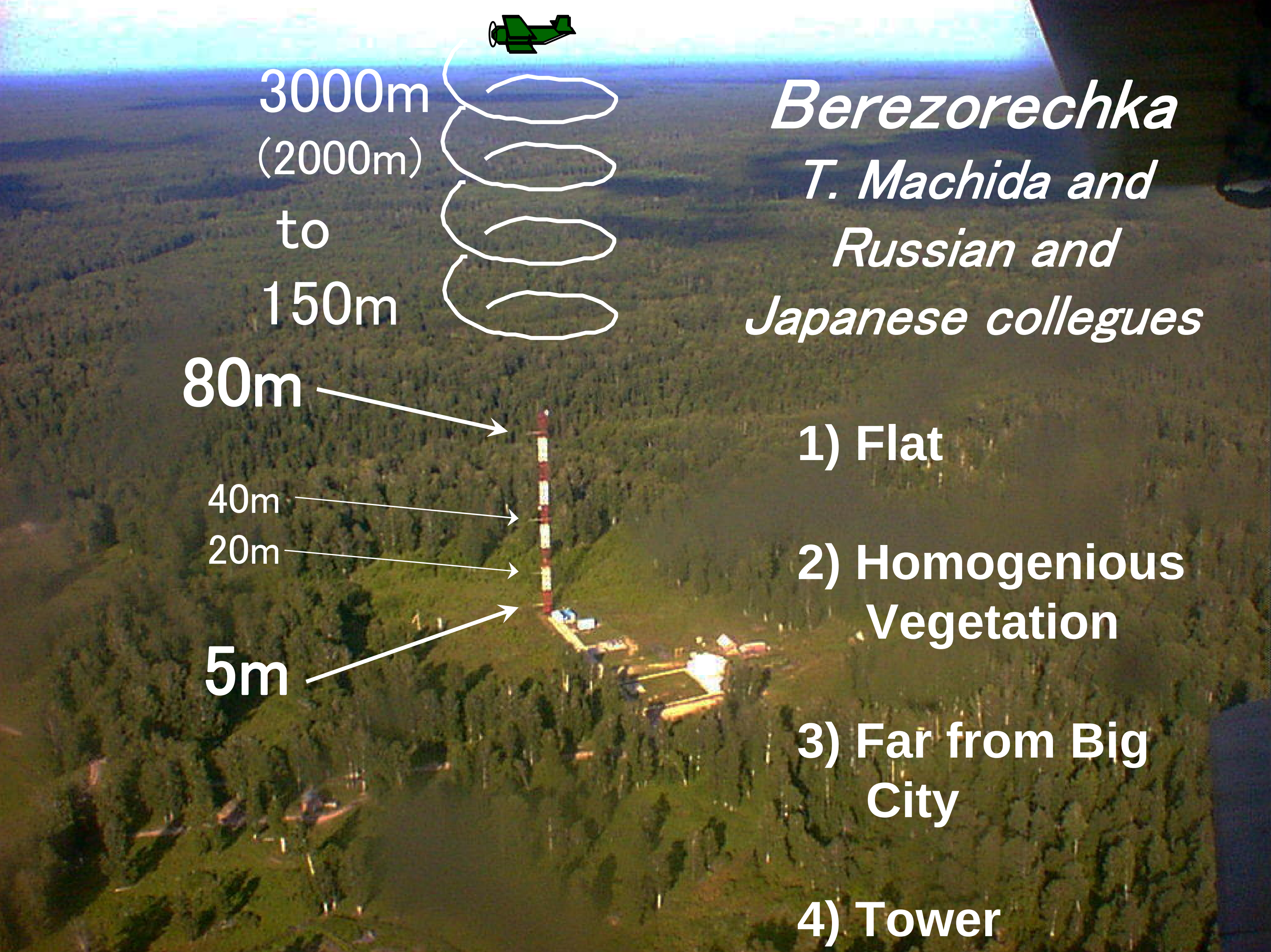

3000m
(2000m)
to
150m
Berezorechka
T. Machida and
Russian and
Japanese collegues
80m
40m
20m
5m
1) Flat
2) Homogenious Vegetation
3) Far from Big City
4) Tower

Berezorechka village, West Siberia

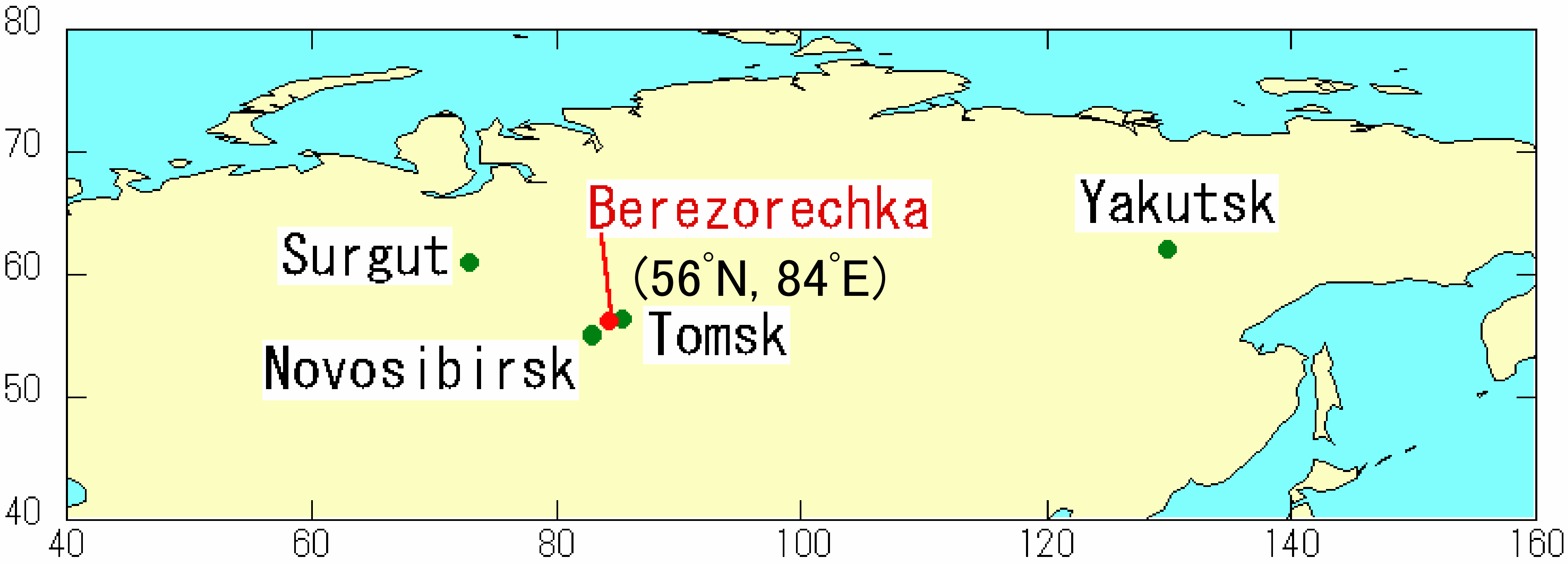

CO2 Measurement System by Air

Small Automatic → High-Frequency Measurement

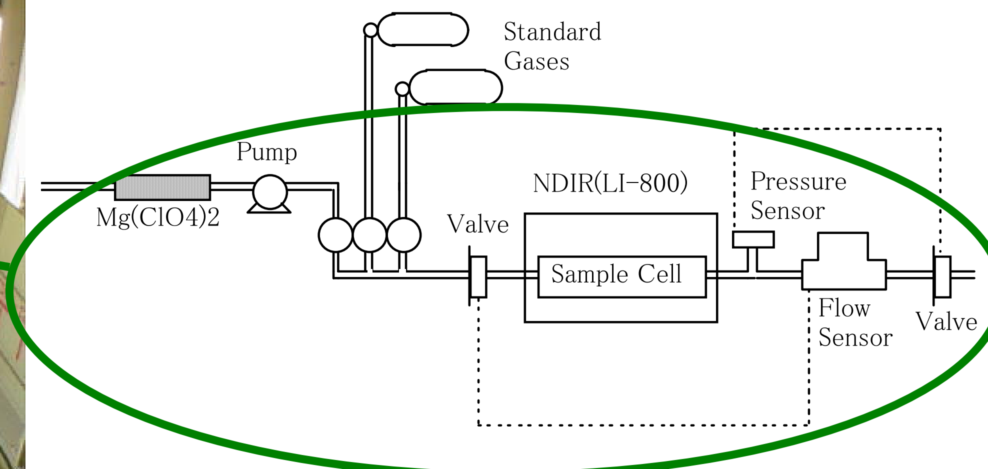

Vertical CO2 profiles in 2002

Oct.'01-Jul.'02

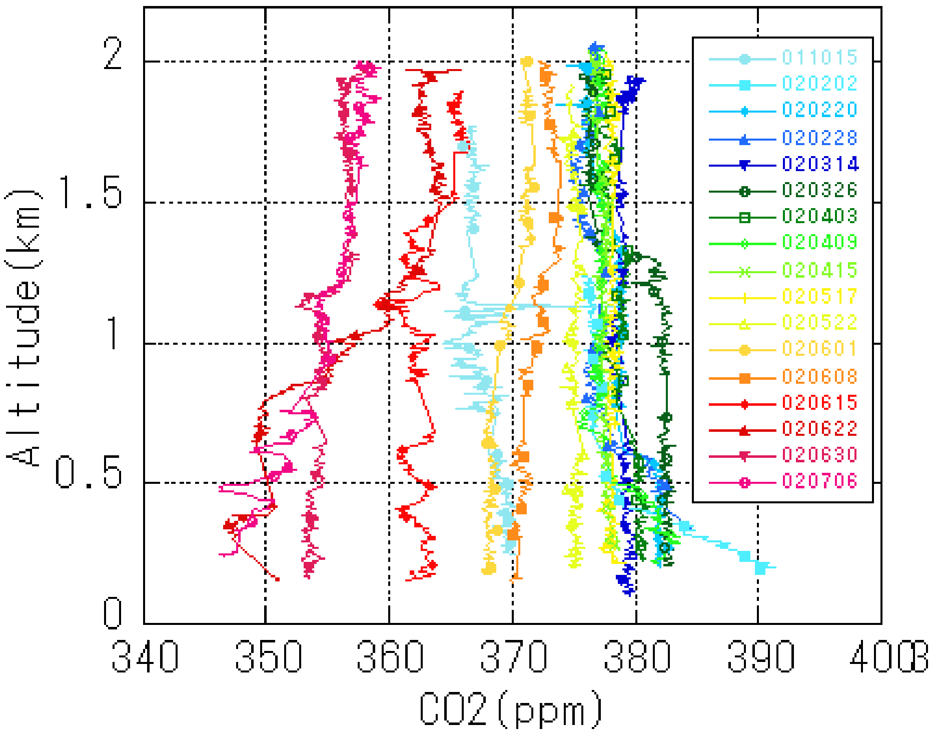

Jul.'02-Dec.'02

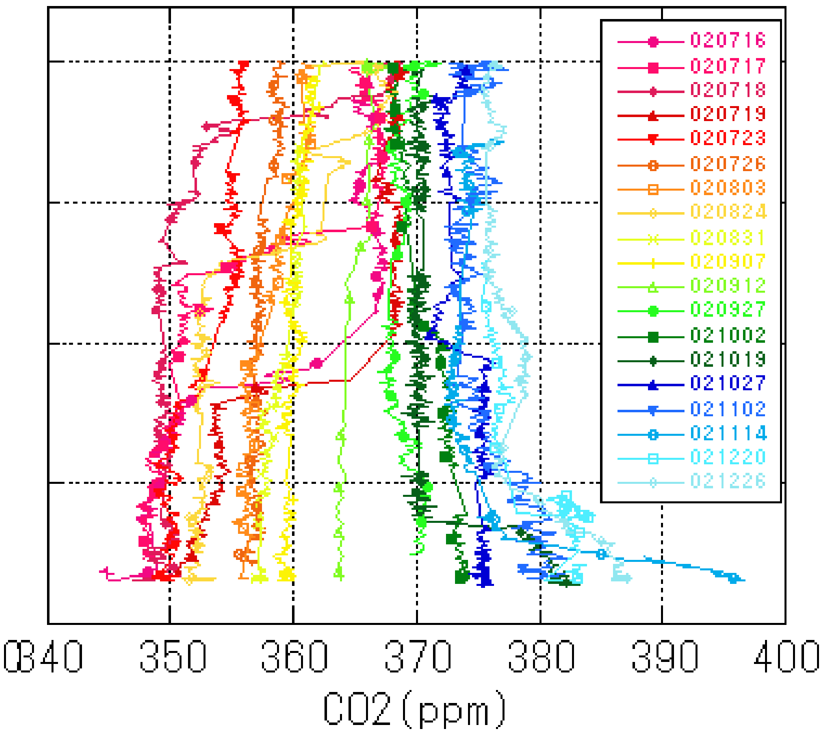

35 Flights in 2002

Vertical CO_2 profiles in 2003

Jan.'03-Jul.'03

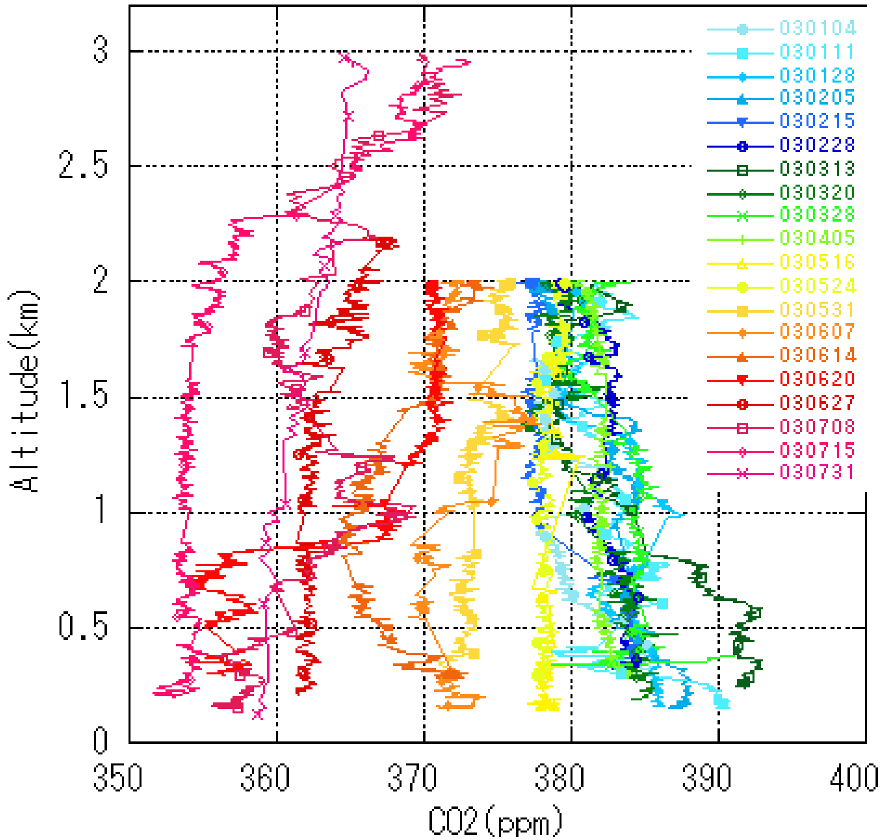

Jul.'03-Dec.'03

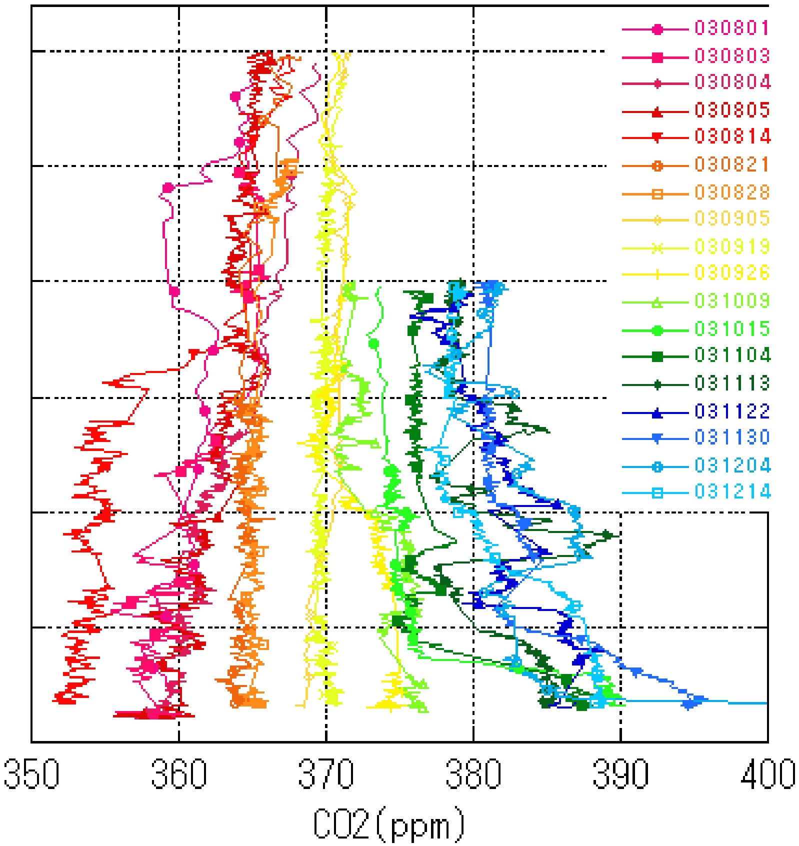

38 Flights in 2003

FT and PBL

26 Mar. 2002

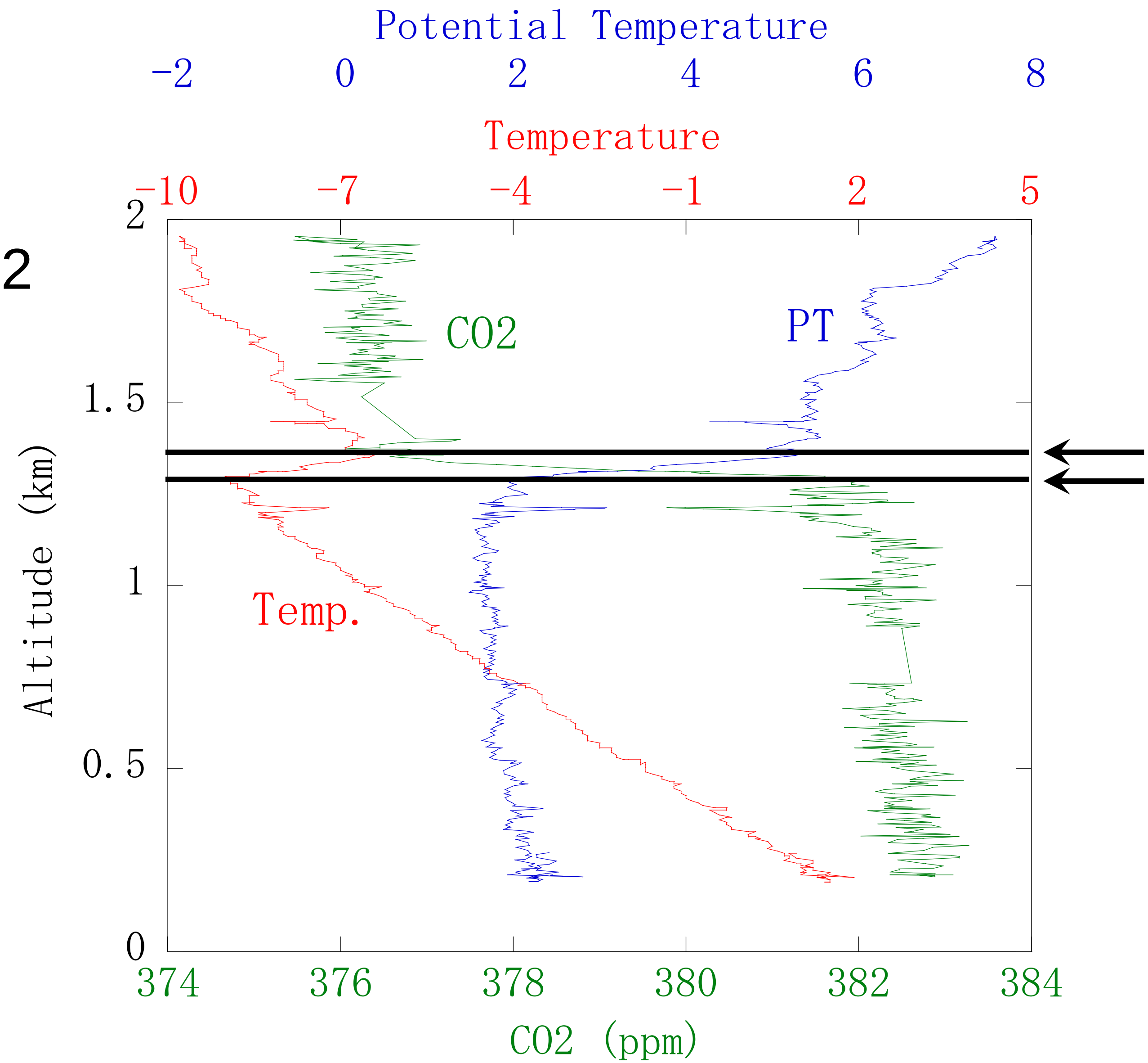

Temporal Variation of CO_2 in FT and PBL

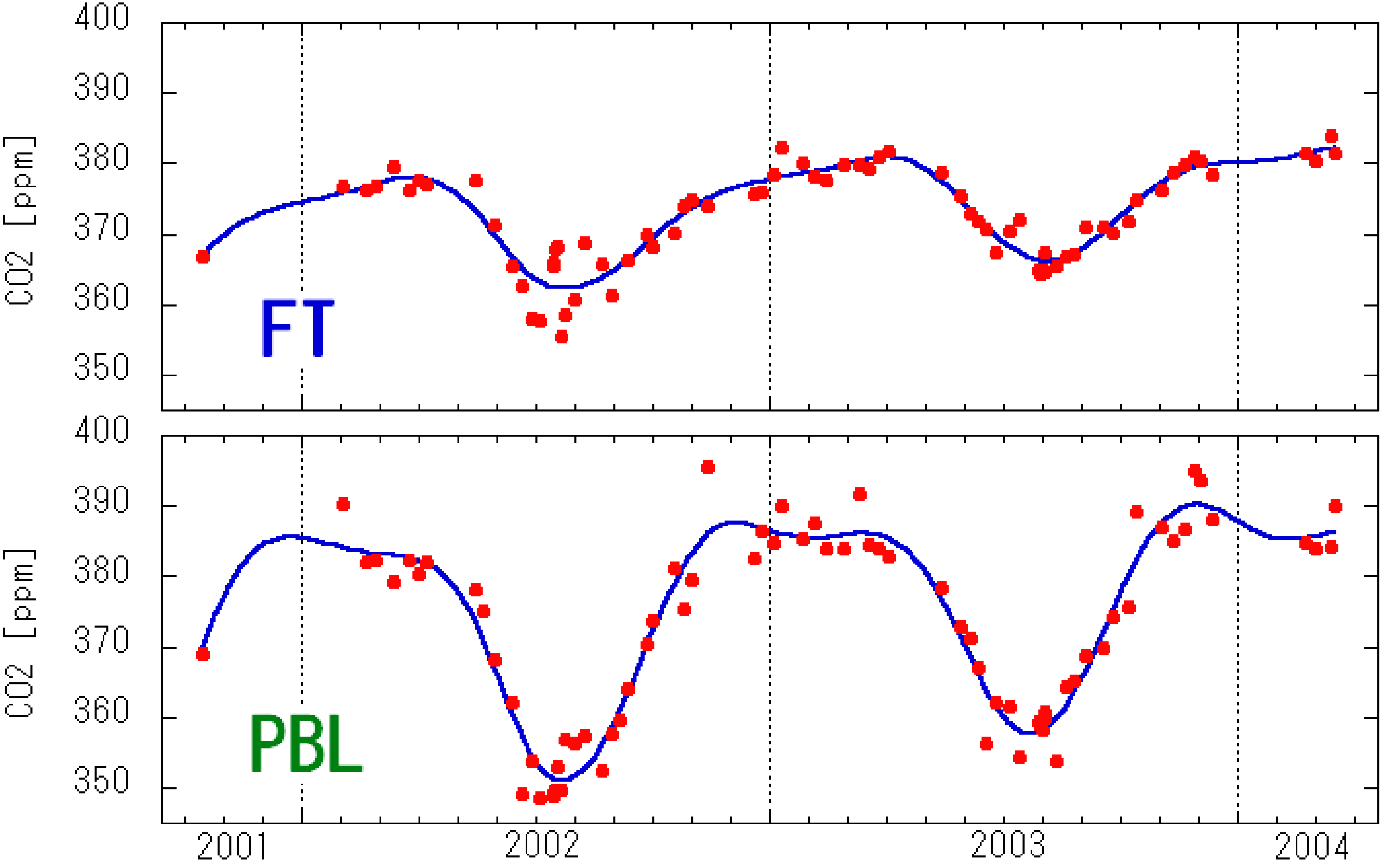

Comparison of Fitting Curves

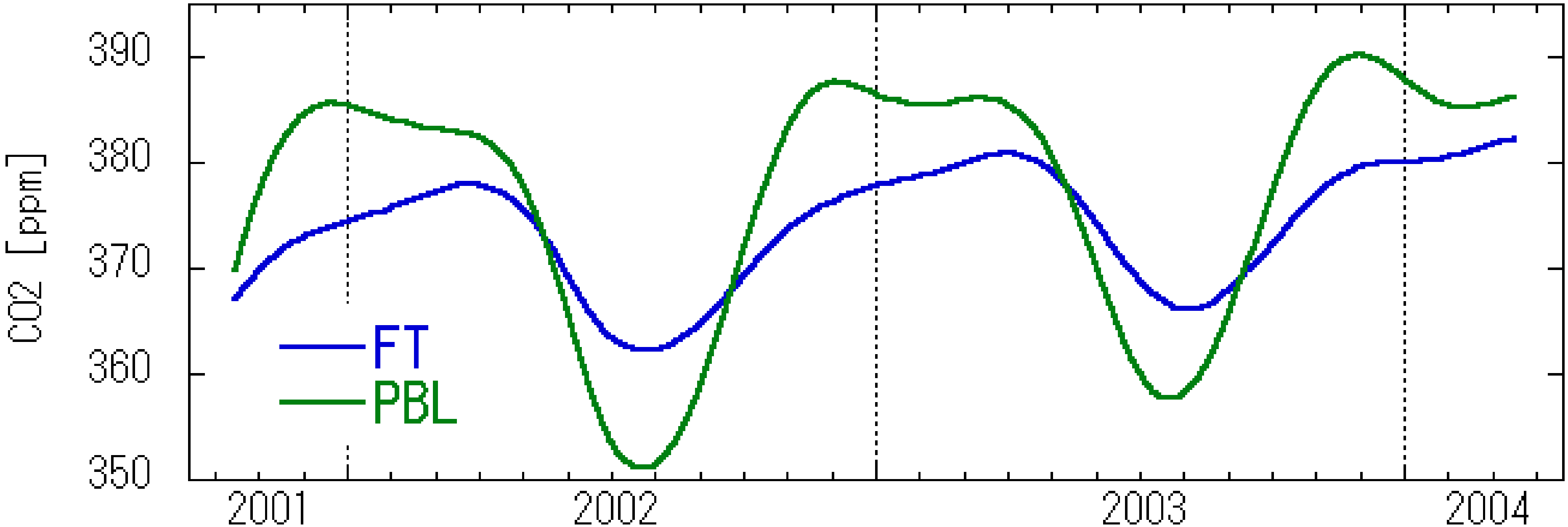

Amplitude = 16ppm(FT) and 34ppm(PBL)
High concentration in Winter
Annual average in PBL is 2ppm higher (rectifier effect)

Comparison between Tower and Aircraft PBL

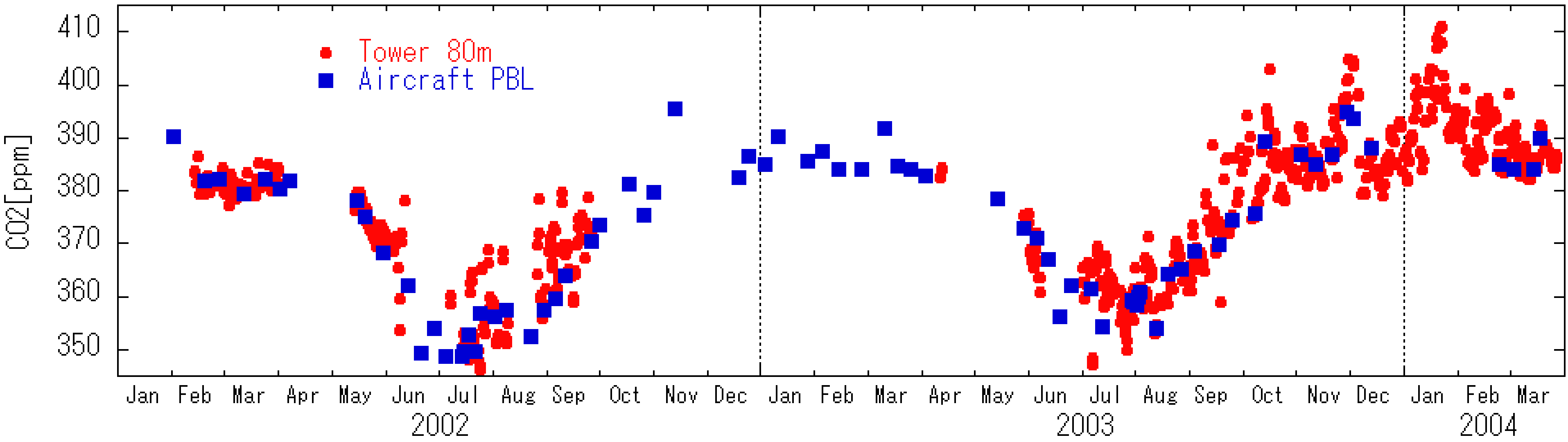

Substantial Difference

-->Aircraft conducts only in the good weather

<u>Weather Bias</u>

Comparison on the good weather condition

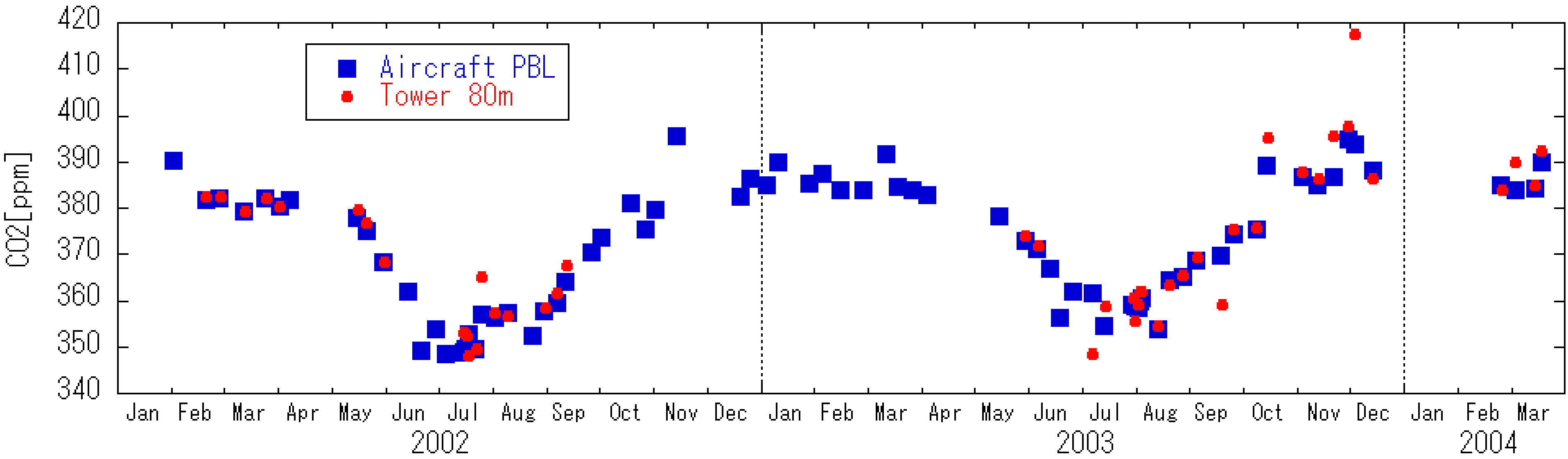

60% data are <+-2ppm

Without Daytime Inversion (Winter)
No Variable day (Summer)

Conclusions

Reconciling orthogonal perspectives

Inversion downscaling

Excellent spatial integration

Strong constraint on flux magnitude

Poor temporal resolution

Limited mechanistic understanding.

Flux tower upscaling

Intrinsically local measurements.

Difficult to upscale flux magnitudes.Variability easier

Excellent temporal resolution

Strong mechanistic understanding

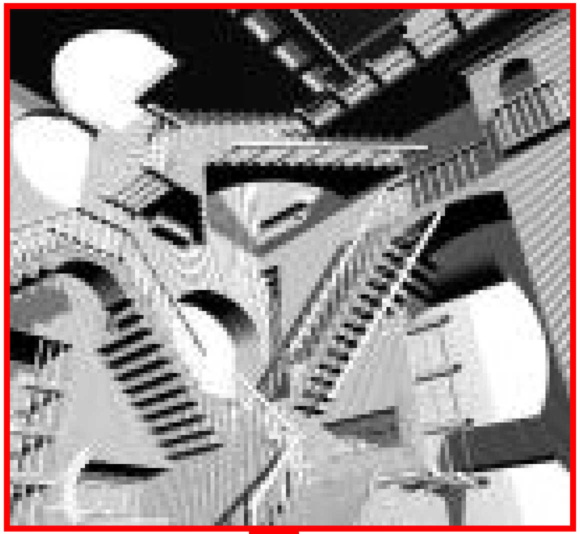

Let's fusion flux upscaling and Inversions !!!

CCDAS,

Coupling of energy budget parameters with transport

Coupling of soil respiration to atmosphere